Review

Synthesis of Metal Organic Frameworks (MOFs) and Their Derived Materials for Energy Storage Applications

Sunil Dutt [1,*,†] **, Ashwani Kumar** [2,*,†] **and Shivendra Singh** [3]

1 Department of Chemistry, Govt. PG College, Una 174303, HP, India
2 Department of Chemistry, Govt. College, Kullu 175101, HP, India
3 Amity School of Engineering & Technology, Amity University Gwalior, Gwalior 474005, MP, India
* Correspondence: sunildutt.iitmandi@gmail.com (S.D.); anshuas1989@gmail.com (A.K.)
† These authors contributed equally to this work.

Abstract: The linkage between metal nodes and organic linkers has led to the development of new porous crystalline materials called metal–organic frameworks (MOFs). These have found significant potential applications in different areas such as gas storage and separation, chemical sensing, heterogeneous catalysis, biomedicine, proton conductivity, and others. Overall, MOFs are outstanding candidates for next-generation energy storage devices, and they have recently attracted the greater devotion of the scientific community worldwide. MOFs can be used to enhance the ability of a device to store energy due to their unique morphology, controllable structures, high surface area, and permanent porosity. MOFs are widely used in super capacitors (SCs), metal (Li, Na, and K) ion batteries, and lithium–sulfur batteries (LSBs) and act as a promising candidate to store energy in an environmentally friendly way. MOFs are also used as efficient materials with better recyclability, efficiency, and capacity retention. In this review, first we summarize the material design, chemical compositions, and physical structure of MOFs and afterward, we highlight the most recent development and understanding in this area, mainly focusing on various practical applications of MOFs in energy storage devices.

Keywords: metal–organic frameworks; synthesis and design; chemical compositions and physical structure; super capacitors; rechargeable batteries; energy storage devices

1. Introduction

Nowadays, materials science research is a very fascinating and important interdisciplinary field that is concerned with the application of various materials in different areas. This area is not new, but the great revolution started in 1995 when Yaghi and co-workers synthesized the first metal–organic framework (MOF) as a special class of porous material that was composed of inorganic metal ions and organic linkers. The MOFs schematic design is shown in Figure 1.
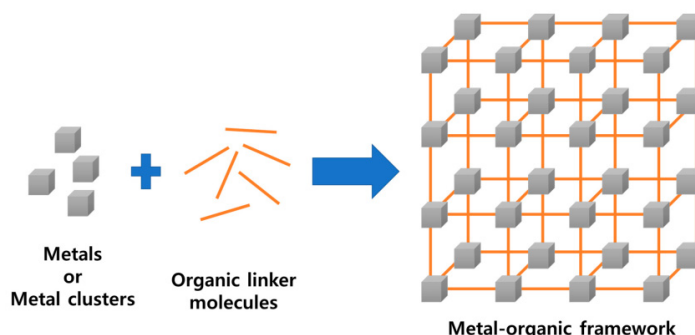

Figure 1. Schematic representation of MOFs [1]. Reproduced with permission.

The term MOF for this new class of materials was also coined by Omar Yaghi in 1995 and has found greater interest of the material and chemical community [2]. MOFs are formed by connecting metal ions or clusters with organic linkers, also called the node-space arrangement [3].The advantages of MOFs compared to traditional materials are their well-regulated structural arrangements. At the molecular level, they possess a highly tunable porosity and surface area by altering metal species and organic linkers, as shown in Figure 2.
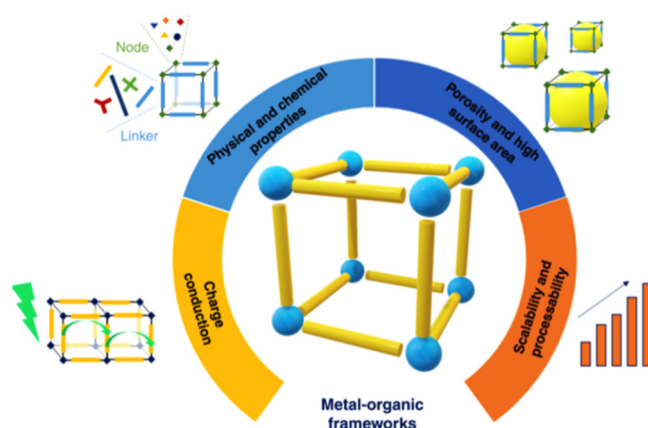

Figure 2. MOFs with tunable porosity, surface area, and charge conduction [4]. Reproduced with permission.

MOFs are remarkably porous inorganic–organic hybrid materials [5] and are designed by the reaction between transition metals and organic ligands with oxygen/nitrogen [6,7]. 1D, 2D, and 3D MOFs have been reported by various research groups and have found potential applications in different areas such as in chemical sensors, catalysis, batteries, supercapacitors, etc. due to their highly tunable pore size, large surface areas, and surface functionalization [8]. Some of MOFs reported by different research groups are shown in Figure 3.

We know that the human survival now a days is hindered by an energy crisis such as the escalating and unpredictable cost of oil, which results in significant increase in the energy requirement globally. This has steadily raised serious problems and also hampers human survival [10]. Highly energy efficient and clean power systems are requirements of the modern era and are urgently needed. If we take a look into the most promising technologies in terms of electrical energy storage, electrochemical energy storage devices such as batteries and supercapacitors came to mind, which have attracted the attention of society because of their light weight, portability, long life cycle, high energy density, and compactness [11,12]. These are widely utilized in mobile phones, computers, environmentally friendly electric/hybrid electric vehicles, portable electronic appliances, aerospace systems, electric vehicles, and many others [12,13]. Overall, the electrode material for an energy storage system is very important, and hence, different researchers have devoted significant effort toward the development of various fascinating materials such as electrode materials for energy storage such as two-dimensional nanomaterial graphene, carbon nanotubes, conducting polymers, nanostructured carbon–polymer composites as well as many others. These materials have their own advantages and disadvantages, for example, polymers are inexpensive and lightweight materials, but due to the lack of their physical and chemical stability, their use is limited. Additionally, inorganic materials are interesting because of their robust structure, but again, mechanical stability is the crucial issue, if we consider their device fabrication [4].

Porosity in materials is very fascinating topic today and hierarchically nanostructured porous materials are much more demanding and useful for energy storage applications due to their large surface area, large accessible space, low density, and excellent accommodation capability [14]. Therefore, various kinds of porous materials are reported in the literature

including conducting polymers, Fe$_2$O$_3$, Sn/C as anodes, porous metal electrodes, porous few-layered MoS$_2$/C nanosheets, etc. [15,16]. Different research groups used various types of porous materials for energy storage applications as shown in Figure 4.
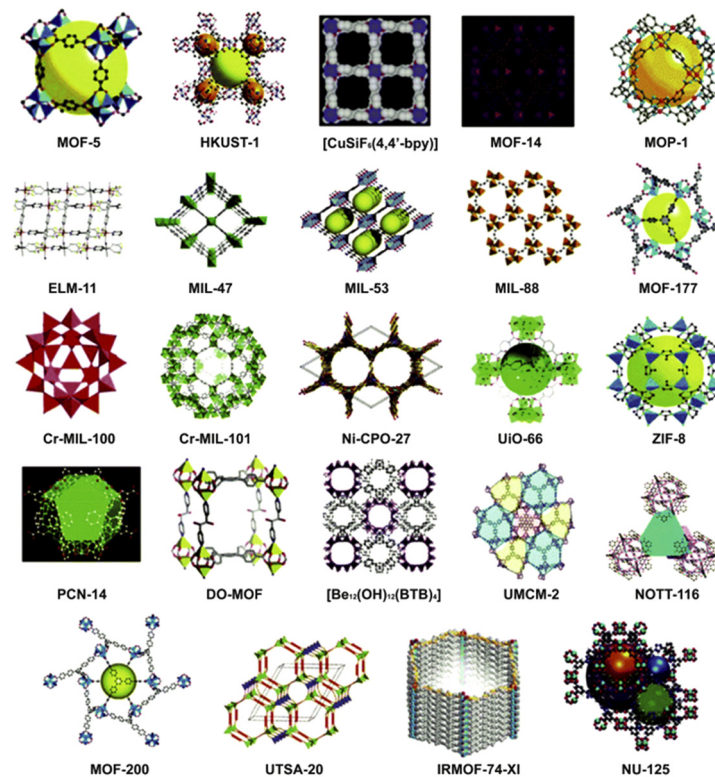

Figure 3. Various types of MOFs synthesized by different research groups [9]. Reproduced with permission.
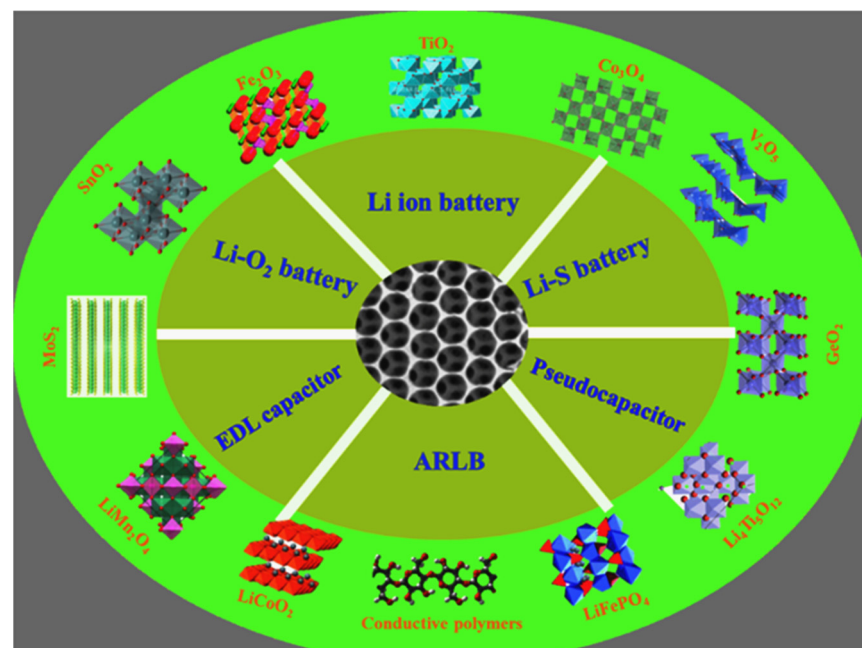

Figure 4. Different types of porous materials used in energy storage applications [16]. Reproduced with permission.

Overall, metal organic frameworks (MOFs) are widely used as emerging and rapidly growing crystalline materials for energy storage applications, which can fulfill the needs of the modern era due to their large surface area, uniform pores with tunability, and the ease of controlling the morphologies and surface properties [17].

2. Different Methods for Synthesis of MOFs

The synthesis of MOFs has attracted immense attention during the last several decades because of their large variety of attractive and exciting structures of great interest for a variety of applications in several fields related to porous materials. These include microwave assisted methods, sonochemical methods, electrochemical methods, mechanochemical methods, the hydrothermal method, solvothermal method, etc. In addition, structure directing solvents and structure directing agents are also used to synthesize the desired MOFs.

2.1. Microwave Assisted Methods

Chang et al. revealed the efficient synthesis of a porous organic–inorganic hybrid material, chromium trimesate, for the first time in 2005 under aqueous conditions [18]. This method is about 20 times faster than conventional methods. Chang's group further demonstrated the rapid synthesis of cubic chromium terephthalate MIL-101 under microwave irradiation in 2007. The synthesized material obtained with giant pores, very large surface areas, and very small nano scale dimensions [19]. The synthesized porous MIL-101 material obtained using this method exhibited a high adsorption of benzene, which makes it a great material for the sorptive removal of harmful organic compounds. Lin et al. demonstrated a similar microwave strategy by using post-synthetic modifications of highly porous NMOFs, with pay loads of imaging contrast agents and anticancer drugs [20]. Jhung's group revealed the synthesis of the most widely studied MOF materials (i.e., chromium-benzenedicarboxylate (Cr-BDC)), named MIL-101. A wide range of reaction conditions such as various water concentrations, pH, and synthetic methods (electric heating and microwave irradiation) have been used to obtain nano-sized crystals [21]. The crystal size of the MOFs decreases with an increase in the concentration of water and pH. This decrease in size with dilution can be explained because of its smaller rate of crystal growth compared to the nucleation rate. Instead of using harmful organic solvents, Horcajada et al. also reported the synthesis of porous iron carboxylate nano MOFs in aqueous or alcoholic solutions [22]. In the biomedical sense, these MOF materials can act as molecular sponges, encapsulating drugs with different polarities and different pore sizes with various functional groups. This modest method has been applied to previously challenging anti tumoral and antiviral drugs, and has also been used as cosmetic agents.

2.2. Sonochemical Method

The synthesis of four well-known MOFs at room temperature was developed by Yaghi et al. in 2008 [23]. Applying the sonochemical method, Yaghi et al. synthesized an isoreticular metal framework (IRMOF) with the cubic topology from acetylenedicarboxylic acid. This kind of MOF has been synthesized by using a special type of reversible fluorescent sensor for size-selective sensing of organoamines by using nanocrystals, as revealed by Qiu et al. in 2008 [24]. The preliminary results as revealed by Qiu's group showed that by the reaction of cupric acetate and H_3BTC, it was possible to synthesize several metal-based MOFs (e.g., $[Cu_3(BTC)_2(H_2O)_3]_n$, a 3-D MOF with 3-Dn channels). Mehring et al. also reported several synthetic procedures to synthesize either $[Cu_3(btc)_2]$ or $[Cu_2(btc)(OH)(H_2O)]$, either starting from $Cu(OAc)_2$ or $Cu(NO_3)_2$ [25].

2.3. Electrochemical Method

A novel electrochemical method for transition metal-based MOFs was revealed for the first time by Mueller et al. in 2005 [26]. The patterned growth of MOFs by applying an anodic voltage to the copper electrode and Cu^{II} ions were introduced by Vos et al. in

2010 [27]. The synthetic solution contained BTC and methyltributylammonium methyl sulfate (MTBS) as a conduction salt. It was established that the densely packed films of $[Cu_3(BTC)_2]$ crystals were easily prepared using electrochemical methods, which also agreed with the thin film X-ray diffractogram. These samples were also in agreement with those of the conventionally prepared reference sample and the literature data. Vos's group further showed a combined method for patterned metallization and galvanic displacement to deposit patterned thin films of MOFs for $Cu_3(BTC)_2$ [28]. Their study also showed that the combination of these methods could advance the processing of MOFs in an easy manner for application in sensors and other thin film applications. The electrochemical method for the synthesis of microporous MOFs was exemplified by the competitive formation of $[Cu_2(btc)_3(H_2O)_3]$ and $[Cu_2(btc)(OH)(H_2O)]$, as revealed by Mehring et al. in 2010 [25]. The electrochemical method for MOF synthesis is shown in Figure 5.
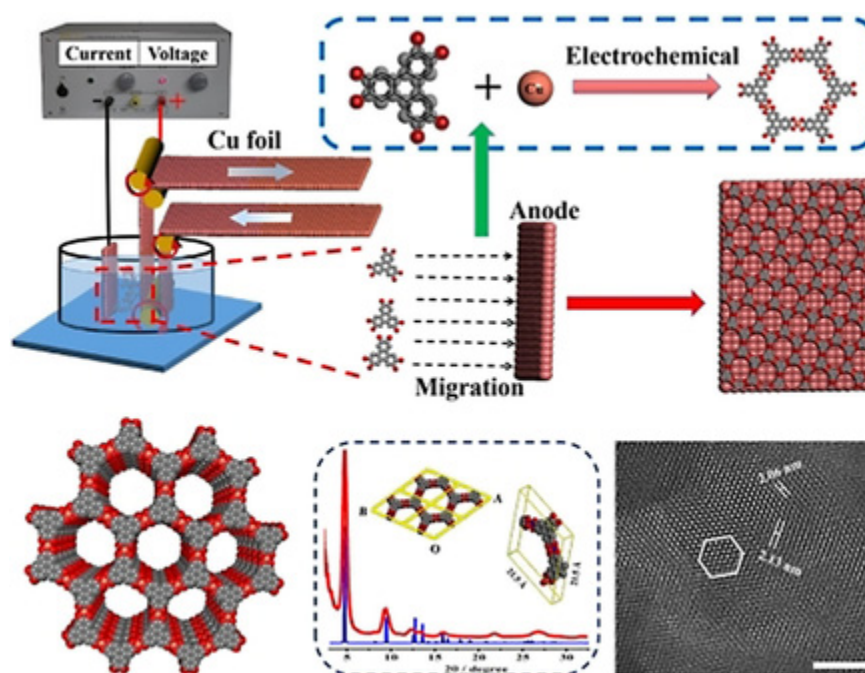

Figure 5. Electrochemical method for MOF synthesis [29]. Reproduced with permission.

2.4. Mechanochemical Method

For the first time, Friscic and Fabian reported the construction of metal–organic polymers from a metal oxide via the liquid assisted grinding approach [30]. This mechanochemical method for the most studied MOFs is shown in Figure 6.

James et al. developed a synthesis of MOFs under grinding conditions by inter conversions between MOF structures induced by liquid-assisted grinding [32]. Furthermore, the solvent-free approach for the synthesis of mixed-ligand materials by grinding MOFs with additional ligands was also revealed by James et al. (Figure 7).

Friscic et al. reported on the ion and liquid-assisted grinding approach for the synthesis of MOFs by the improved mechanochemical method in 2010 [33]. The method revealed LAG reactions at the 0.5 mmol scale by placing a mixture of ZnO (40 mg), Hta (80 mg), and DABCO into a 10 mL stainless steel jar, along with DMF as the grinding liquid and two stainless steel balls using 1–20 mg salt.
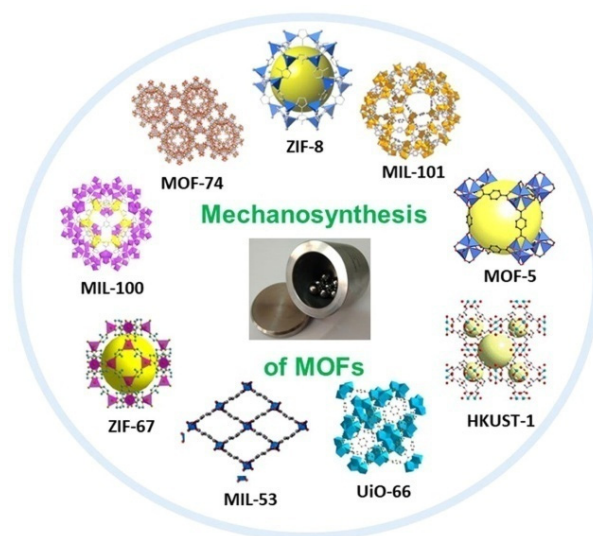
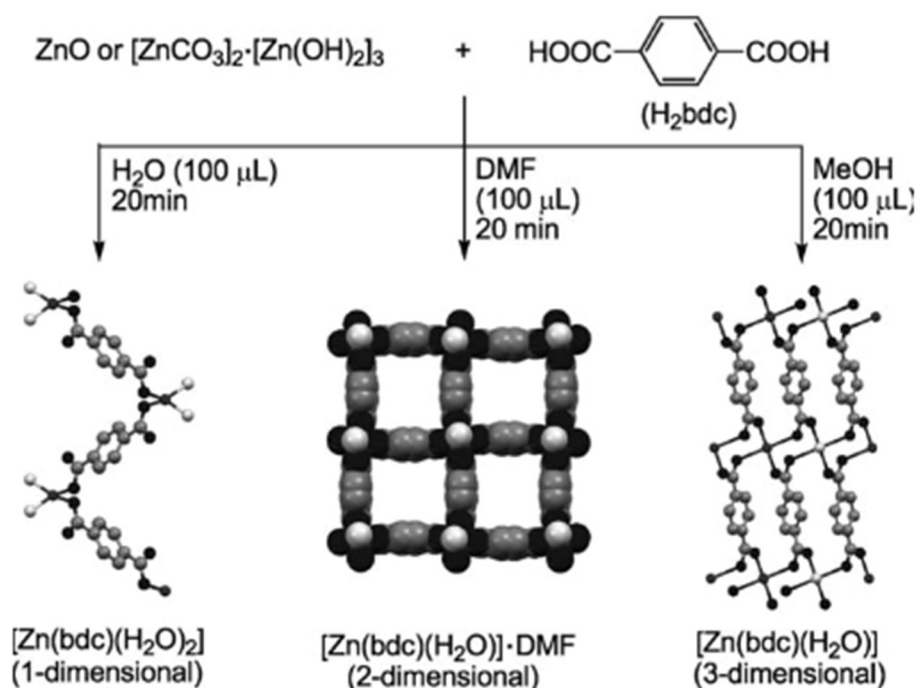**Figure 6.** Different MOFs synthesized using the mechanochemical method [31]. Reproduced with permission.

Figure 7. Synthesis of MOFs using liquid-assisted grinding (LAG) [32].Reproduced with permission.

2.5. Hydrothermal Approach

In 2006, Loiseau et al. reported the synthesis of a new aluminum trimesate compound: $Al_{12}O(OH)_{18}(H_2O)_3(Al_2(OH)_4)[btc]_6$, $24H_2O$ by using aluminum nitrate with 1,3,5-benzenetricarboxylic acid and a linker in water media by applying the hydrothermal approach [34]. In aluminum chemistry, this wasthe first time that such a μ_3-oxo-centered trinuclear configuration was observed. The same group also revealed the synthesis of new indium trimesate $In_{12}O(OH)_{12}(\{OH\}_4,\{H_2O\}_5)[btc]_6$. $31H_2O$, called MIL-96, (btc = 1,3,5-benzenetricarboxylate or trimesate species) and gallium trimesate $Ga_{12}O(OH)_{12}(\{OH\}_4, \{H_2O\}_5)[btc]_6.24H_2O$ under mild conditions hydrothermally in the presence of trimethyl 1,3,5-benzenetricarboxylate [35–37]. Furthermore, Gao et al. showed that the assembly of the asymmetric bis(bidentate)-2-pyrimidinecarboxylate ligand with Cd^{II} produced a MOF with the RHO zeolitic topology, while 5-(20-pyrimidyl)tetra-zolate with Cd^{II} led to

square grid networks [37]. Xu et al. synthesized two microporous yttrium trimesates with different spatial arrangements of the linkers around the Y^{3+} centers, but having similar 1-D channels from yttrium salt and trimethyl 1,3,5-benzenetricarboxylate via the insitu hydrolysis reaction in mixed solvents of DMF/water and DEF/water [38]. The microporous 3D MOF, $[Cu_3(ipO)_2(pyz)_2]_n$ was synthesized by the in situ ligand transformation in a hydrothermal approach using $Cu(NO_3)_2 \cdot 2.5H_2O$, 1,2,3-benzene tricarboxylic acid (H_3btc), pyrazine, KOH, and water [39].

2.6. Solvothermal Approach

Using high-throughput methods, for the first time in 2008, Stock et al. reported a solvothermal method for the preparation of isoreticular structures of different MOFs based on Fe(III) and aminoterephthalate [40]. The reactions of $FeCl_3$ and 2-aminoterephthalic acid under suitable conditions in both protic and aprotic solvents were studied. Using high-throughput methods, Stock's group also revealed the preparation of the Al-based MOF $[Al_4(OH)_2(OCH_3)_4(H_2N\text{-}bdc)_3] \cdot xH_2O$ (CAU-1) with high porosity and thermal stability. The structure contains unprecedented octameric $\{Al_8(OH)_4\text{-}(OCH_3)_8\}^{12+}$ building units that are connected through the aminoterephthalate ions to a 12-connected net [41]. Li's group investigated the synthesis of MOFs in aqueous media using metallic chromium, which was dispersed in an aqueous solution of HF. After adding H_3BTC, the mixture was dissolved in a mixed solvent of water/methanol in equal proportion. The resulting mixture was heated in a Teflon autoclave at 210 °C for 4 days, which furnished a green powder and was further washed with distilled water followed by methanol and then dried in air [42].

3. MOF Applications in Energy Storage Devices

The energy crisis issues seriously threatening human survival because alternative sources of energy such solar energy and wind energy are fluctuating sources of energy. Therefore, the design of the electrodes is the main task for efficient electrochemical capacitors, rechargeable batteries, fuel cells, and electrolyzers [43]. Similarly, MOFs are also outstanding electrode materials for electrochemical energy storage devices that meet the needs of next-generation energy storage technologies such as in Li-S/Se batteries, LIBs, SIBs, Li-air batteries, and supercapacitors. This is due to their exceptional morphology, suitable functional linkers, high specific surface area, and metal sites. Therefore, due to high energy efficiency and clean power systems, electrochemical energy storage devices are much more demanding such as batteries and supercapacitors, and this research area has rapidly been extended [44–46]. Batteries are used in various electronic gadgets such as portable electronic devices due to their low weight, high energy density, and SIBs and LIBs are regarded as a low-cost alternative battery technology [47–51]. Long cycle life, high power density, and the competitive price of supercapacitors has also made them a significant candidate for energy storage, and thus used in electric vehicles and aerospace systems [52,53]. MOFs offer various advantages due to their unique structure and are promising materials due to their porous structure with a large surface area in energy storage and conversion. The properties of the MOFs also depend on their structure and have been investigated very well in the literature by different research groups. Different MOFs such as MIL-53, MIL-68, MIL-125, UiO-66, ZIF have been prepared. It was found that they exhibit different morphology, pore size, and surface chemistry, and showed different water adsorption behavior [53] Furthermore, it showed different isotherms for different samples and MIL-68 showed a reversible extreme "S" shape isotherm [54]. The specific structural features and flexibility of MOF structures also affects their adsorption properties. MOFs do not follows Gurvitsch's rule, which controls the adsorption properties and hence the extent of adsorption. Gating and kinetic trapping processes are very unique to flexible MOFs, which are very important for adsorption purposes [55]. The extraordinary inherent properties of MOFs make it a potential candidate for various technologies [56]. Appropriate linkers with different lengths and various metal nodes can be used to tune up the pore size and topology of the framework, which has an impact on the electrochemical

process [57]. Metal–oxygen linkages make up the MOF insulator, but the conductivity can be improved using "through-bond" conductivity, which directly deals with the tuning of morphology using the metal–sulfur bond [58]. Spatial and directional transport control can be tuned using polar functionalities into the framework [59]. Charge conduction and sulfur adsorption can be enhanced by tuning the morphology of MOFs because the diffusion length can be shortened by decreasing the particle size for better conversion [60]. In this section, the recent developments, future prospectives, and challenges of MOFs for energy storage applications are summarized. MOFs find potential applications in Li-S, Li-Se, supercapacitors etc as shown in Figure 8.
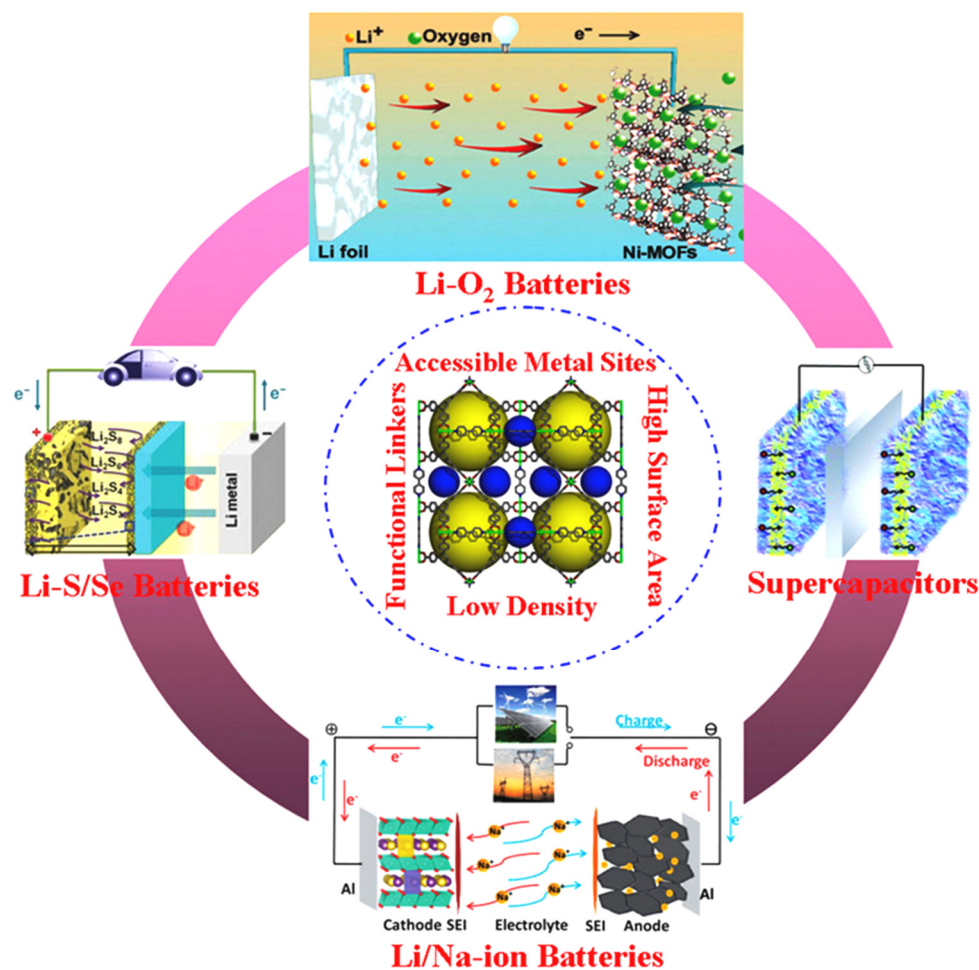

Figure 8. MOFs in energy storage and conversion devices [61]. Reproduced with permission.

3.1. MOFs in LIBs

Currently, the importance of electronic gadgets and other electronic materialshas increased rapidly. High performance LIBs are widely used in various electronic gadgets such mobile phones, laptops, and electric automobiles, etc. as energy storage batteries with better performance. Thus far, a variety of materials has been explored for better performance in LIBs as anode/anode materials, MOFs also being among them. The MIL-53(Fe) can be directly used as a cathode electrode material by inserting lithium ions and was synthesized in 2007 by using the solvothermal process by Tarascon et al. [62].

If we talk in terms of the high capacity, these LIBs are the best materials, as they consume very low energy. The increasing demand for a high energy capacity has not been fulfilled by other materials, for example, graphite, which has a theoretical capacity of 372 mA h g^{-1}. Instead, a different solvothermal method was used to synthesizeCo-based metal–organic framework (H–Co–MOF) microflowers, which showed a superior capacity of

1345 mA h g^{-1} with aa current density of 0.1 A g^{-1} after 100 cycles. Moreover, this material showed a large capacity of 828 mA h g^{-1} after 700 cycles at 2 A g^{-1} [63]. H–Co–MOF and Co–MOF cycling performance for LIBs is shown as in Figure 9.
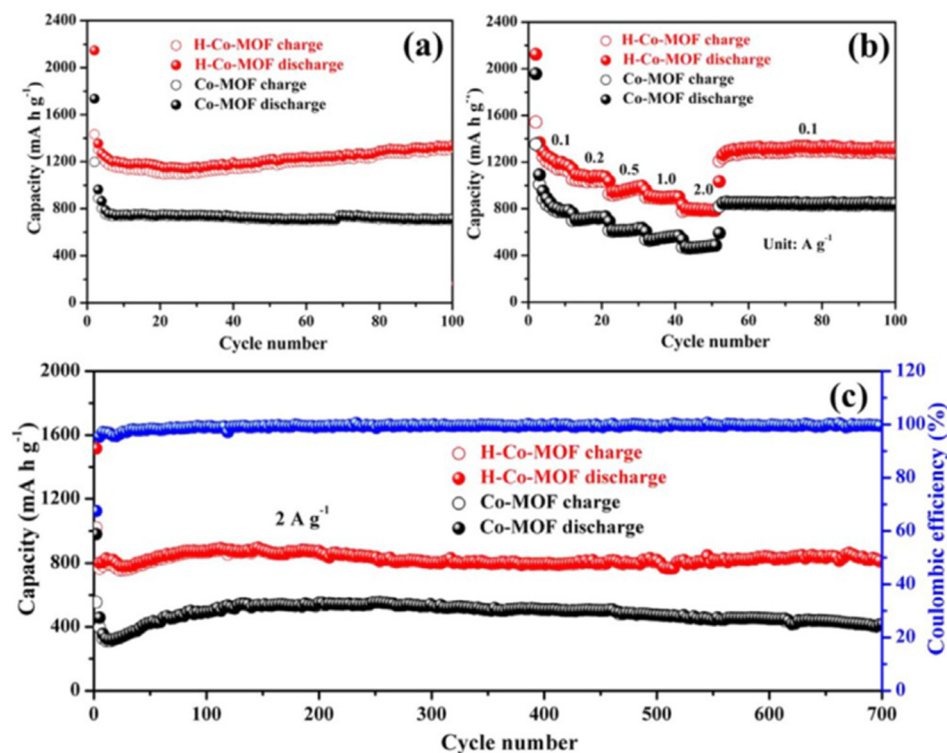

Figure 9. (**a**) H-Co-MOF and Co-MOF cycling performance at a current density of 0.1 A g^{-1}, (**b**) rate capability, and (**c**) long-term cycling performance at a current density of 2 A g^{-1}, respectively [63]. Reproduced with permission.

MOF can be used to obtain different porous carbon materials, as shown in Figure 10. A high specific capacity and an extensive life cycle can be obtained with a MOF-derived porous carbon material.
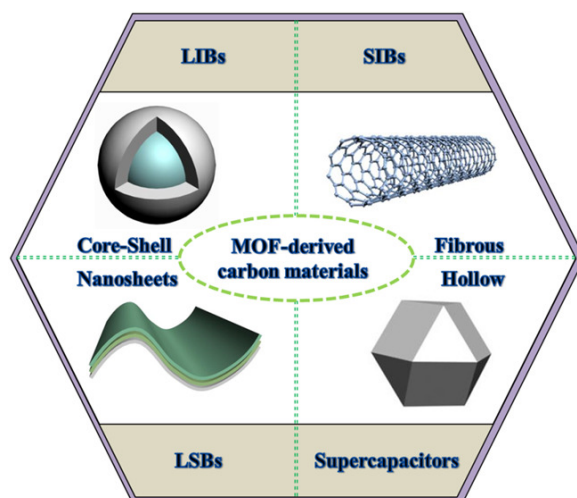

Figure 10. MOF-derived carbon materials for energy storage applications [64]. Reproduced with permission.

MOF-177 [Zn$_4$O(1,3,5-benzenetricarboxylic acid)] showed a capacity of 400 mA h g^{-1} in the first cycle to 105 mA h g^{-1} after two cycles. This decrease in capacity has arisen

because the Zn-based MOF electrode undergoes a conversion reaction and alloying reaction [65]. Additionally, the theoretical capacity of ZnO is987 mA h g^{-1} and it is considered as one of the most satisfactory anode materials due to its low cost and environmentally friendly nature, but the main drawback of this material is the low electrical conductivity and large volume expansion [66]. Therefore, this problem with ZnO nanoparticles is overcome by hollow porous ZnO/C nanocages, which showed a first discharge capacity of 1982 mA h g^{-1} (current density of 100 mA g^{-1})and 1178 mA h g^{-1}after 100 cycles, as shown in Figure 11, and the capacity was 351 mA h g^{-1} at a current density of 2 A g^{-1} [67].
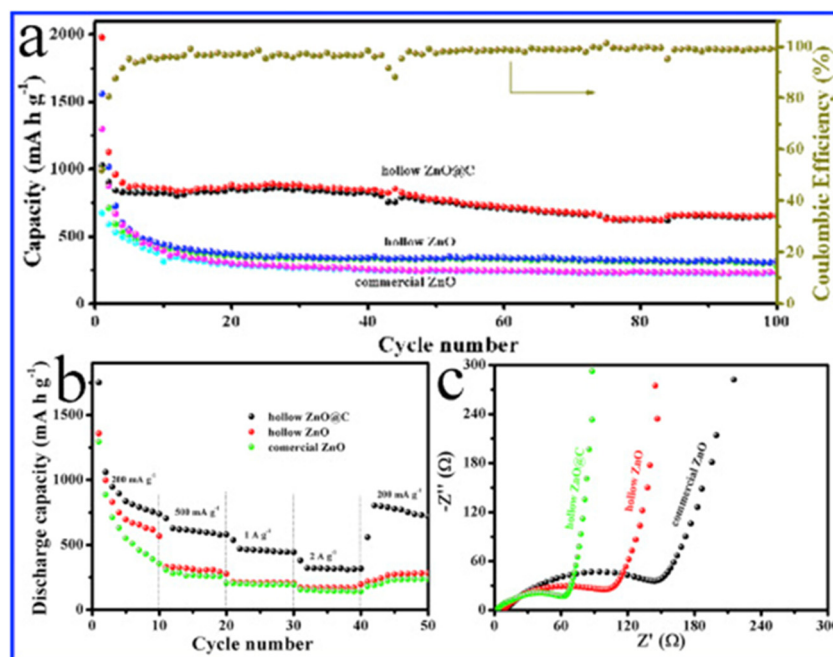

Figure 11. (**a**) Capacity of hollow ZnO/C, hollow ZnO, commercial ZnO (**b**) Charging/discharging capacity (**c**) impedance spectra of same materials [67]. Reproduced with permission.

Several polymetallic Li–MOFs such as MnLi, CoLi, NiLi, MnCoLi, MnNiLi, CoNiLi, and MnCoNiLi were prepared using the hydrothermal method [68]. The best electrochemical performance was exhibited by MnCoLi with a discharge capacity of 799.4 mAh g^{-1} after 100 cycles (current density of 100 mA g^{-1}). Electrochemical performance of MnLi, CoLi, NiLi, MnCoLi, MnNiLi, CoNiLi, and MnCoNiLi is as shown in Figure 12.

A flexible and wavy layered nickel-based MOF ($C_{20}H_{24}Cl_2N_8Ni$) was synthesized by the solvothermal approach of 3,3′,5,5′-tetramethyl-4,4′-bipyrazole (H_2Me_4bpz) with nickel(II) chloride hexahydrate as shown in Figure 13.

It was also investigated whether the material $C_{20}H_{24}Cl_2N_8Ni$ showed excellent specific capacity, cycling performance, and preservation of the crystal structure as shown in Figure 14. The synthesized MOFs showed a first discharge specific capacity of 320 mAhg^{-1}, and the second discharge specific capacity dropped to 140 mAhg^{-1}. Specific capacity loss of 56.25% was observed for this MOF [69]. This loss was observed due to the SEI layer being caused by the incomplete conversion reaction and irreversible lithium loss.
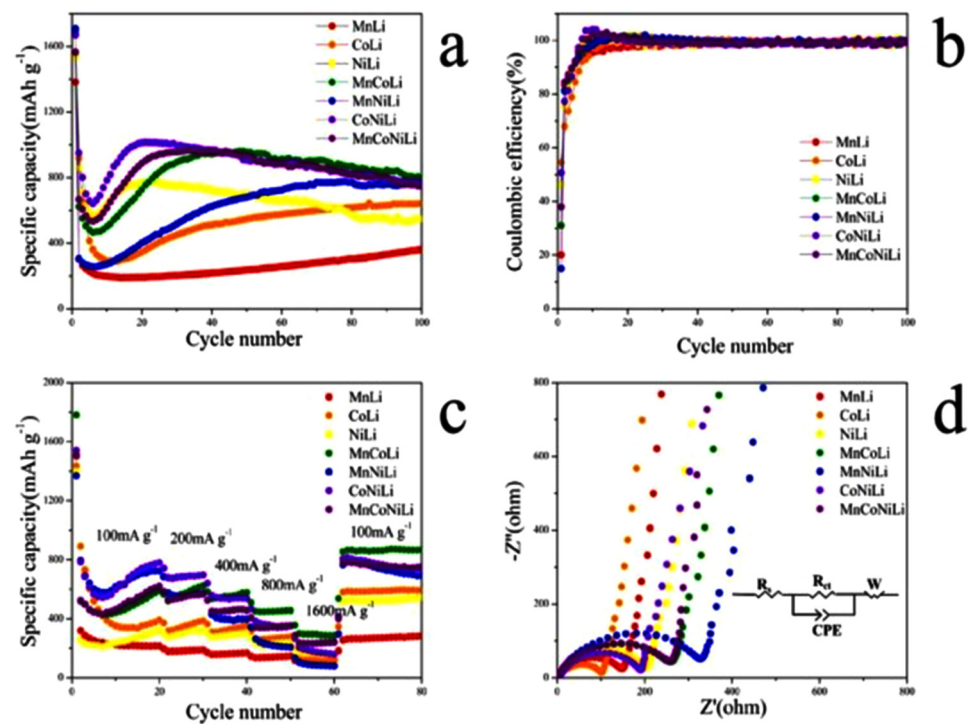
Figure 12. Electrochemical performance of MnLi, CoLi, NiLi, MnCoLi, MnNiLi, CoNiLi, and Mn-CoNiLi: (**a**) Cycling performance and (**b**) Coulombic efficiency of the electrodes at 0.1 A g^{-1}; (**c**) rate capabilities at various current densities; (**d**) EIS spectra of cells before cycling [68].Reproduced with permission.
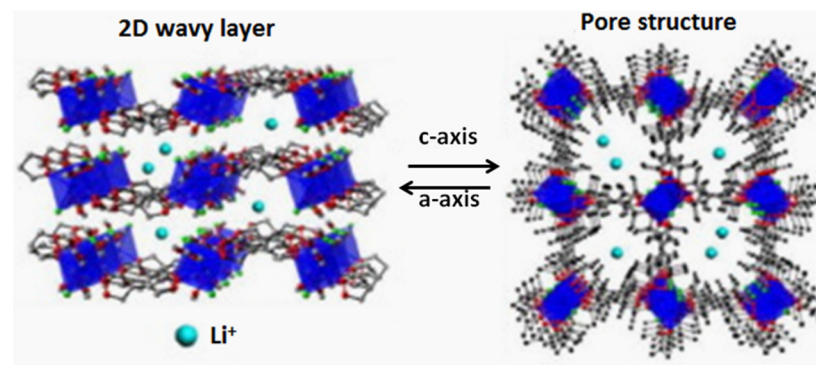

Figure 13. 2D layered nickel-based MOF ($C_{20}H_{24}Cl_2N_8Ni$) [69]. Reproduced with permission.
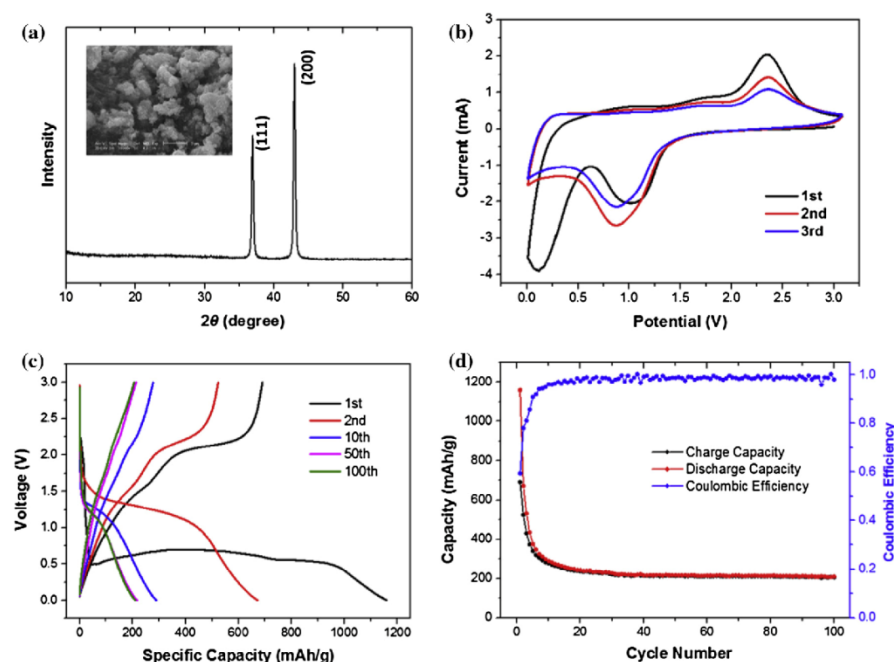
Figure 14. (**a**) Crystal structure, (**b**) CV, (**c**,**d**) Performance of $C_{20}H_{24}Cl_2N_8Ni$ MOF [69]. Reproduced with permission.

3.2. MOFs in Sodium Ion Batteries (SIBs)

Sodium ion batteries (SIBs), because of their low cost, have a higher demand due to their rapid use in the development of electric vehicles and consumer electronics for a variety of commercial applications. SIBs can work at ambient- or room-temperature without any problem and they are currently gaining much attention. Additionally, sodium is very abundant with low cost, and special attention has been of it. In SIBs, sodium ions migrate, but in LIBs, the lithium ions migrate, but the basic component and structure of SIBs are identical to that of the LIBs [70–72]. Carbon electrodes were used in the beginning, but transition metal oxide-based electrodes replaced carbon electrodes [73]. Later on, porosity was introduced into the materials for electrodes for a better cycle life of the SIBs, but unsatisfactory results were found in terms of reversible capacity [74]. Thus, the problem was mostly solved with MOFs, and efficient electrodes were designed based on it and its derivatives for SIBs [75]. Ni–metal–organic framework (Ni–MOF)-derived nickel sulfide (NiS_2) was used as the electrode material and it showed a high specific capacity and excellent rate performance in the SIBs. Ni–MOF-derived NiS_2 electrodes showed the discharge capacity of 579.3, 362.7, 334.3, 330.9, and 280.6 mA h g^{-1} for the 1st, 3rd, 5th, 10th, and 60th cycles, respectively [76] as shown in Figure 15. The discharge specific capacity of the electrode for SIBs was very high, and could reach a value of 186.9 mA h g^{-1} after 100 cycles with a 76.2% retention value.

Likewise, the scalable solution-precipitation method was used to prepare MOF, 2-methylimidazole zinc salt (ZIF-8), followed by pyrolysis, which resulted in microporous carbon (ZIF-C) with a homogeneous pore size of 0.5 nm. It has been shown that ZIF-C has a better performance than the other CMK-3 electrodes. The initial charge capacities shown by the electrodes with ZIF-C and CMK-3 were 164 and 95 mA h g^{-1}, respectively. This capacity was retained even after increasing the current density to 500 mA g^{-1}, 129, and 56 mA h g^{-1}, which showed an exceptional storage behavior for SIBs [77]. MOFs have been studied as electrode materials for aqueous sodium-ion rechargeable batteries (ASIBs) due to them being cheap, safe, and of low toxicity [78] as shown in Figure 16.
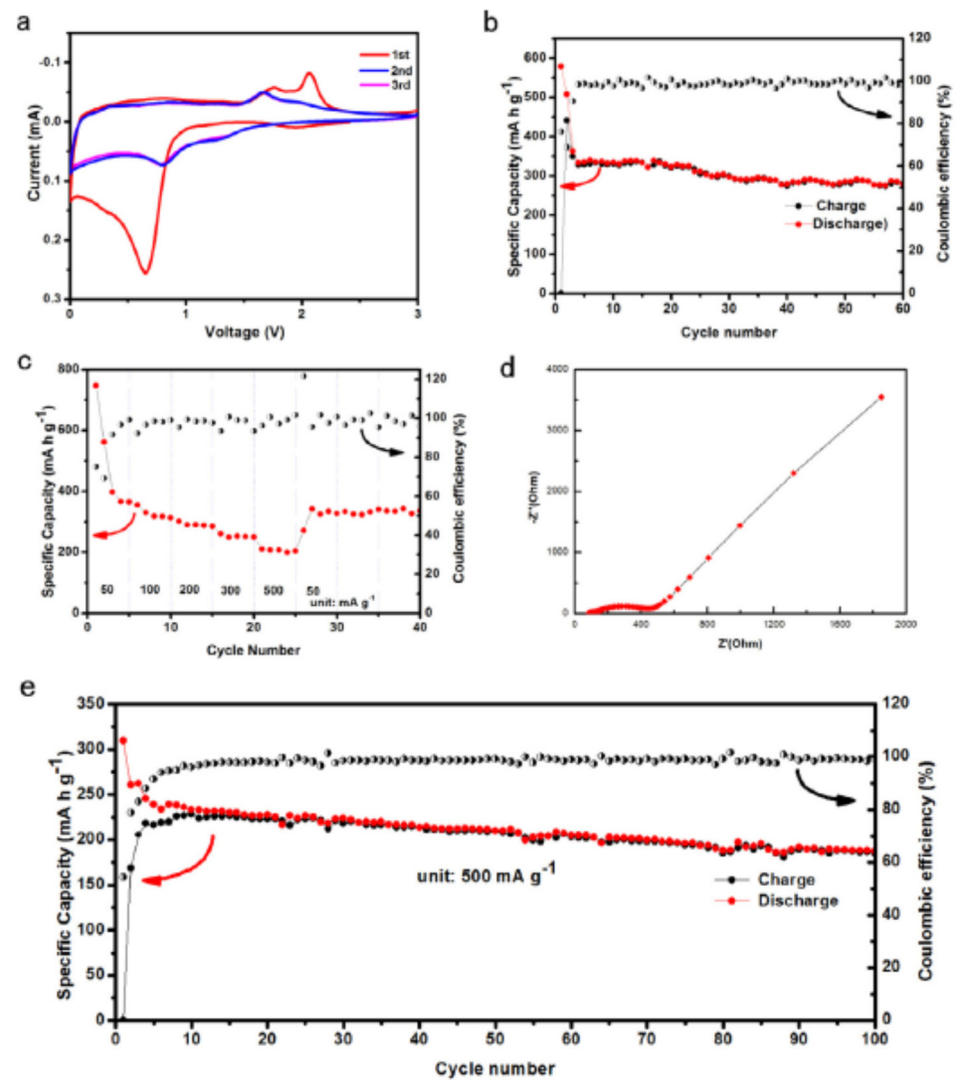
Figure 15. (**a**) CV at a scan rate of 0.05 mV s^{-1}. (**b**) Cyclic performances of the NiS$_2$ anode at 100 mA g^{-1}. (**c**) Rate performances of the NiS$_2$ anodes. (**d**) Nyquist plots of the NiS$_2$ electrodes. (**e**) Cycling performance of the electrode at a high current density of 500 mA g^{-1} [76]. Reproduced with permission.

Figure 16. MOFs as electrode materials for aqueous sodium-ion rechargeable batteries (ASIBs) [78]. Reproduced with permission.

Similarly, simple carbonization of MOF-5 led to the preparation of cube-shaped porous carbon (CPC) with a large surface area of 2316 m^2g^{-1}, which showed a better sodium-storage capacity of 240 mA h g^{-1} at a current density of 100 mA g^{-1} after 100 cycles. Even after 5000 cycles 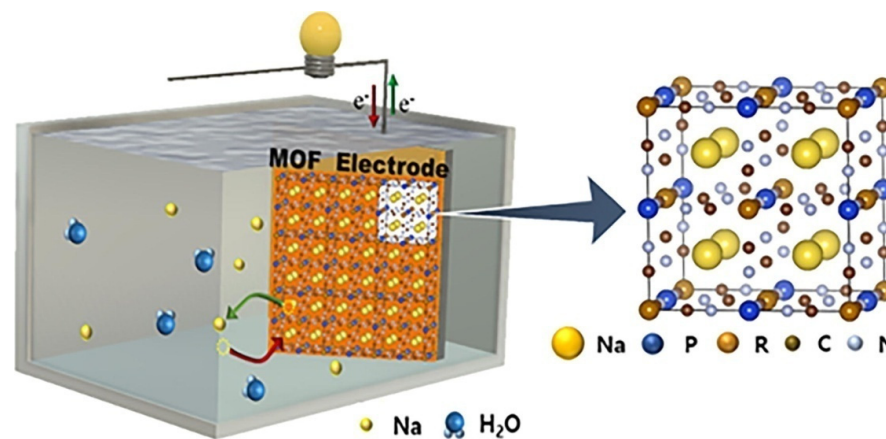at the current density of 3200 mA g^{-1}, the high specific capacity of 100 mA h g^{-1} was still retained [79]. Furthermore, flexible MOF based electrodes were also used as the superior electrode and they showed superior energy storage performance with good rate capability, a reversible specific capacity of 82 mA h g^{-1} at 0.2C, and long cycle life with 81.2% capacity withholding over 1000 cycles [80]. A new metal–organic framework prepared using the solvothermal method is $\{(Me_2NH_2)_2[Co_3(\mu_3\text{-}O)(btb)_2(py)(H_2O)]\cdot(DMF)_2(H_2O)_2\}_n$ (Cobtbpy). H_3btb is defined as 1,3,5-tri(4-carboxylphenyl)benzene, py = pyridine, DMF = N,N-dimethylformamide). The (3,6)-connected to a 3D network with a point symbol of $(4\cdot6^2)_2(4^2\cdot6^{10}\cdot8^3)$ based on the $[Co_3(\mu_3\text{-}O)]$ clusters was shown by Cobtbpy. This material can be used in SIBs due to its stability, accessibility, and dense active sites. A composite mixed with CNTs can also be used as an anode material with high reversible capability, delivering 379 mAh/g in sodium-ion batteries at 0.05 A/g [81]. A scalable 2-D MOF via the solvothermal method was thoroughly investigated as high-performance anodes for SIBs $[Co(L)(H_2O)]n\cdot2nH_2O$ [defined as "Co(L) MOF"] and $[Cd(L)(H_2O)]n\cdot2nH_2O$ [defined as "Cd(L) MOF"] (L = 5-aminoisophthalic acid) [82]. Porous TiO_2 derived from MOFs (MIL-125) showed excellent sodium ion storage performance with high capacity, good cycling stability, and excellent rate performance with a maximum capacity of 250 mAh g^{-1} at the current density of 50 mA g^{-1} after 50 cycles. A capacity of 173 mAh g^{-1} was still retained at a high current density of 1 A g^{-1}, even after 2500 cycles [83]. Annealing of a Mn-based metal–organic frameworks precursor was used to synthesize porous MnO@C nanorods. A high reversible specific capacity of 260 mAh g^{-1} after 100 cycles at a current density of 50 mA g^{-1} was achieved using this hybrid material. MnO@C exhibited a superior long-life cycling performance with a capacity of 140 mAh g^{-1} at very high current density of 2 A g^{-1} [84], as shown in Figure 17.
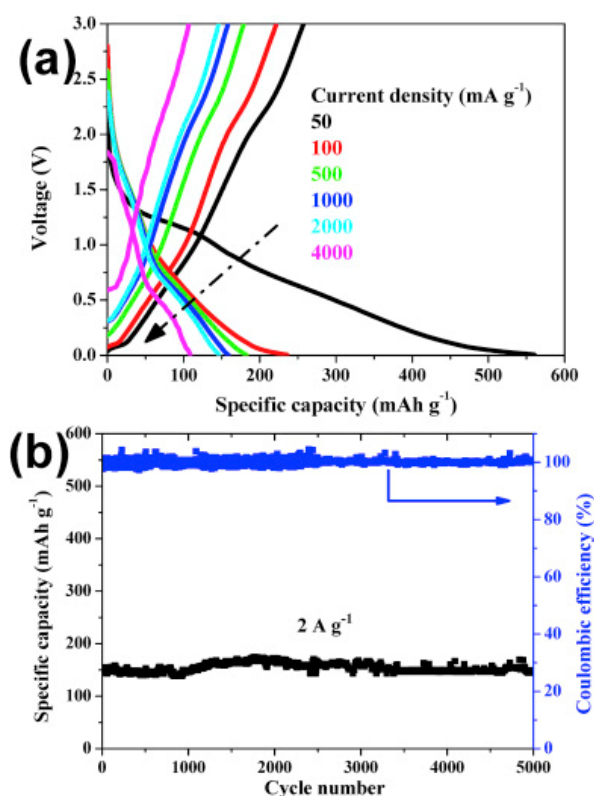

Figure 17. Electrochemical performance (**a**) Voltage vs specific capacity (**b**) Specific capacity vs cycle number of the MnO@C nanorods derived from metal–organic frameworks as the anode in SIBs [84]. Reproduced with permission.

It was investigated whether the substitution of the Cu nanoparticles in a metal–organic framework (MOF)-derived octahedron carbon framework was used to prepare ultrafine antimony embedded in a porous carbon nanocomposite (Sb@PC). This material was synthesized using the insitu method and showed excellent performance in SIBs. The specific capacities of 634.6, 474.5, and 451.9 mAh g^{-1} at 0.1, 0.2, and 0.5 A g^{-1} after 200, 500, and 250 cycles, respectively, were excellent, with a suitable redox potential in the range 0.5–0.8 V vs. Na/Na$^+$ shown by this material [85]. Moreover, a MOF was used in the synthesis of a 3D porous carbon (3DPC) material that possessed a high specific surface area and large pore volume and has been used in high-performance sodium ion batteries. An excellent reversible capacity of 284 mAh g^{-1} was achieved even after 100 cycles. The same material showed a better rate capability with a high reversible capacity of 125 mAh g^{-1}, even at a high current density of 2.5 A g^{-1} and robust long-term cycling stability for upto 3000 cycles with a marvelous capacity of 175 mAh g^{-1} at 1 A g^{-1} [86]. A wide range of materials has been reported by different research groups for applications in SIBs. Hydrolysis, followed by the ion exchange method and subsequent calcinations, led to the formation of $MgFe_2O_4$ microboxes. An easy pathway for the insertion/extraction of Na$^+$ was provided by sufficient space and the diffusion pathway. This material showed a capacity of 406 mA h g^{-1} at a current density of 50 mA g^{-1} and up held a reversible capacity of 135 mA h g^{-1} upto 150 cycles, as shown in Figure 18.
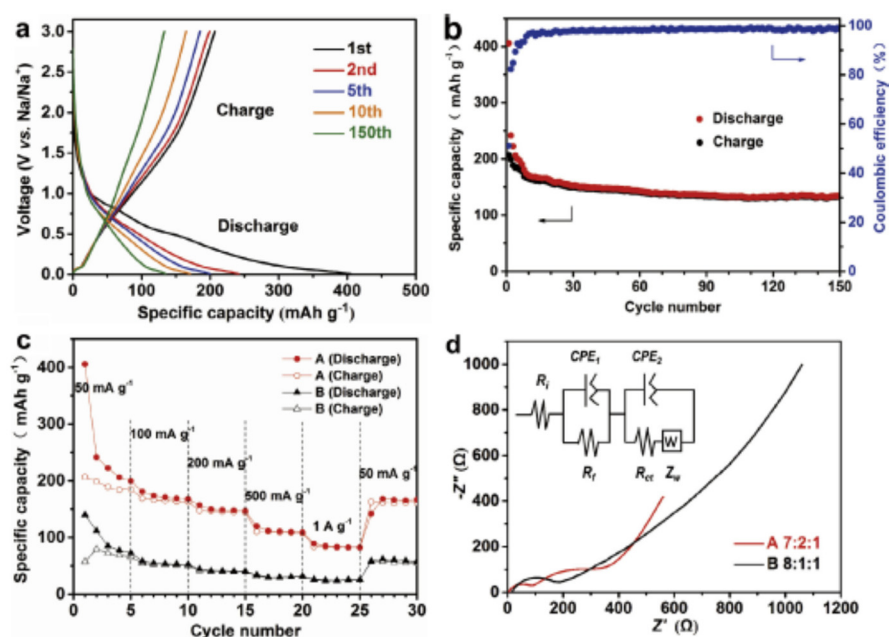

Figure 18. Various active material ratios of A (7:2:1) and B (8:1:1) were used to check the electrochemical performance of the $MgFe_2O_4$ microbox electrodes. (**a**) Charge/discharge curves and (**b**) cyclic performance of sample A at a current density of 50 mA g^{-1}; (**c**) rate performance, and (**d**) Nyquist plots of samples A and B [87]. Reproduced with permission.

3.3. MOFs in Li–O₂ Batteries

MOFs have attracted the great attention of the scientific community as an electrode material in lithium–oxygen (Li–O₂) batteries, sometimes called lithium air batteries. These batteries are made up of lithium metals, which act as the anode, along with porous carbon composites that act as the cathode. It has been studied that these rechargeable lithium–air batteries have the highest theoretical specific energy among rechargeable batteries and are also capable of transforming energy to a practical device. Moreover, MOFs have been well-studied and used in various kinds of heterogeneous catalysis for many reactions with Li–O₂ batteries in ORR and OER [88].

3.4. MOFs in Li–S Batteries

Similar to other batteries, lithium–sulfur (Li–S) batteries have found a potential application in aerospace systems and electrical equipment. The theoretical specific energy density is 3 to 5 times higher than that of Li ion batteries, and they are supposed to be used in next-generation energy storage systems at larger scale [89]. The high capacities of secondary batteries have been developed by using new conversion type batteries such as Li–S batteries. These batteries generate electrical energy by the chemical redox of sulfur (S_8) because of its remarkable potentialities in energy storage [90].

3.5. MOFs in Li–Se Batteries

In recent years, lithium–selenium (Li–Se) batteries have been given a lot of attention because of their outstanding performances and high theoretical volumetric energy densities (~3253 mAh cm^{3-}). These Li–Se batteries, when compared to Li–S batteries, show an improved rate and cycling performance over Li–S batteries. However, these Li–Se batteries have many challenges compared to other batteries. For example, in the process of the lithiation of selenium, the cathode experiences huge volume expansion due to the void space in its lattice spectrum. Instead, selenium possesses high conductivity compared to sulfur (S_8). Moreover, in these batteries, MOFs have been used as a pyrolysis precursor to create porous carbon frameworks [91].

3.6. MOFs in Super Capacitors (SCs)

Yaghi et al. used a different series of MOFs with several organic ligands and different central metal ions, which showed a high areal specific capacitance [92]. The electrochemical double layer (EDL) mechanism or faradaic mechanism are the two mechanisms in which to store electrical energy in electrochemical capacitors. These are based on the mechanism wherein the former process, the EDL layer is formed by the electrolyte ions on the surface of the electrode, and in the latter case, by redox reactions involving the surface regions of the electrode materials [93]. MOFs are well-utilized in the field of supercapacitors as electrode materials, but a low capacity has limited their use in supercapacitor applications. The first neat MOF-based supercapacitor without conductive additives or other binders was explored by Sheberla et al. in 2016 [94]. Zn-based metal–organic frameworks (MOFs) were used to prepare nanoporous carbon, which was used in symmetric supercapacitors because nanoporous carbon has a high specific surface area, good capacitance (specific capacitance of 251 F g^{-1} in 1 M H_2SO_4), high stability, and good rate capability [95]. The Ag–MOF electrochemical performance is shown in Figure 19.
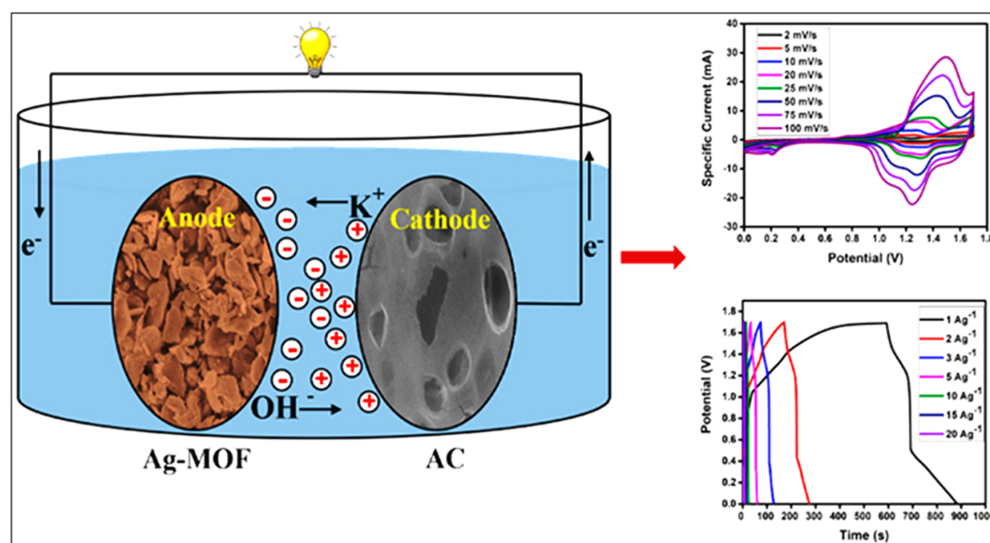

Figure 19. Schematic representation and electrochemical performance of the silver–MOFelectrode material in the supercapacitors [96]. Reproduced with permission.

The electrochemical double-layer capacitance (EDLC) at the enlarged specific surface area of the materials can be raised by using mixed metal–organic frameworks (M–MOFs). The conductivity and specific surface area of MOFs can be improved using mixed central metal ions. The Co/Ni–MOF//CNTs–COOH also exhibited an excellent energy density (49.5 W·h·kg^{-1}) and power density (1450 W·kg^{-1}). In these MOFs, the conductivity was improved by substituting Ni^{2+} in the Ni–MOF with Co^{2+} or Zn^{2+} by a simple hydrothermal method [97]. The electrode electrochemical performances of the Zn/Co–MOF-derived material is shown as in Figure 20.
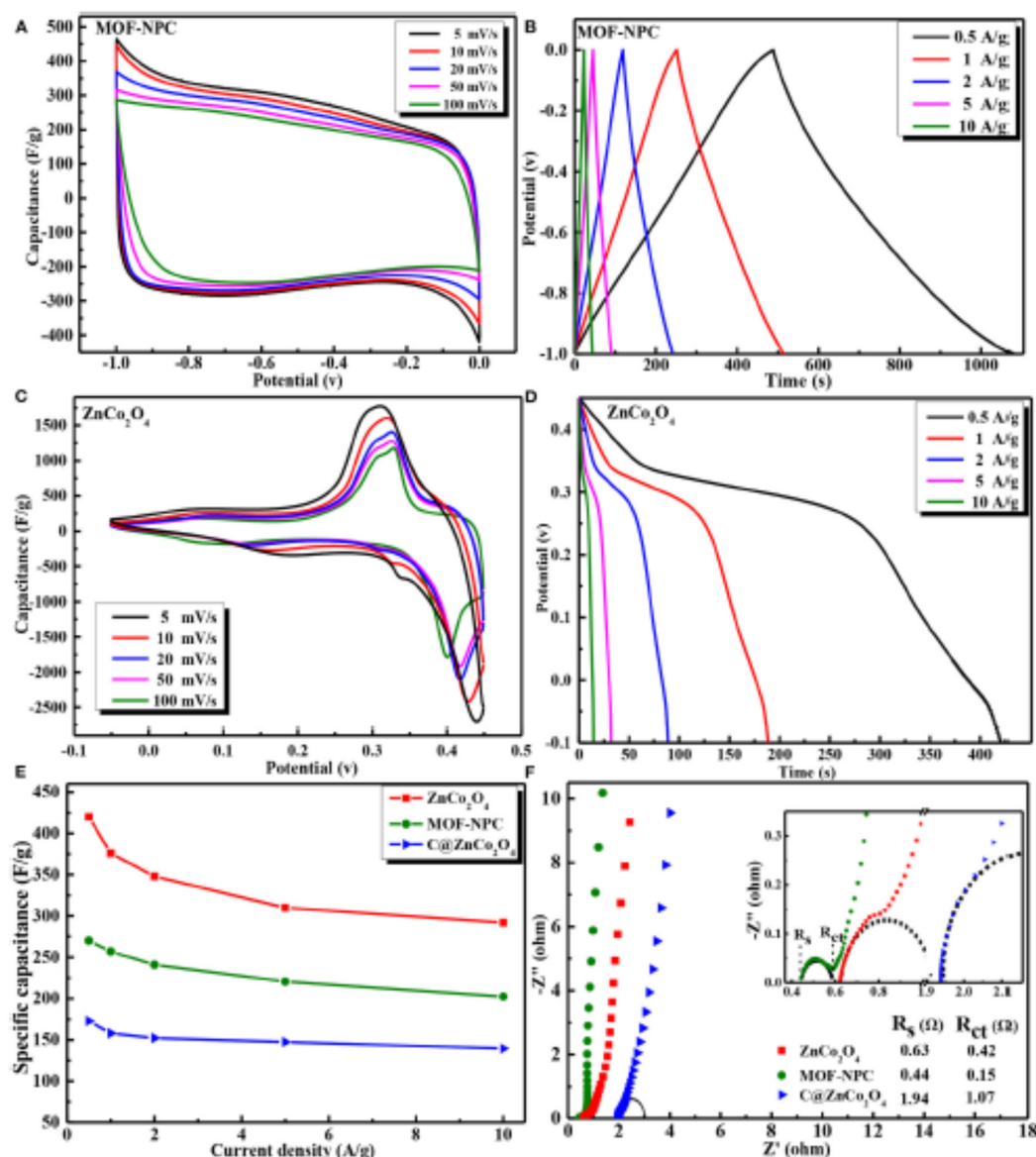
Figure 20. The electrode electrochemical performances of the Zn/Co–MOF-derived material: CV curves at various scan rates of (**A**) MOF-NPC and (**C**) ZnCo$_2$O$_4$; GCD curves at various current densities of (**B**) NPC and (**D**) ZnCo$_2$O$_4$. (**E**) Specific capacitance at different current densities of MOF-NPC, C@ZnCo$_2$O$_4$, and ZnCo$_2$O$_4$. (**F**) EIS curves of MOF–NPC, C@ZnCo$_2$O$_4$, and ZnCo$_2$O$_4$ [98]. Reproduced with permission.

Co8–MOF-5 (Zn$_{3.68}$Co$_{0.32}$O(BDC)$_3$(DEF)$_{0.75}$),designated as Co8–MOF-5, was used as the electrode material, which showed a better performance in energy storage [99]. PANI-ZIF-67-CC-based MOFs are used in SCs effectively because the bulk electric resistance of

MOFs becomes reduced and it exhibits an extraordinary areal capacitance of 2146 mF cm^{-2} at 10 mV s^{-1}, as shown in Figure 21 [100].
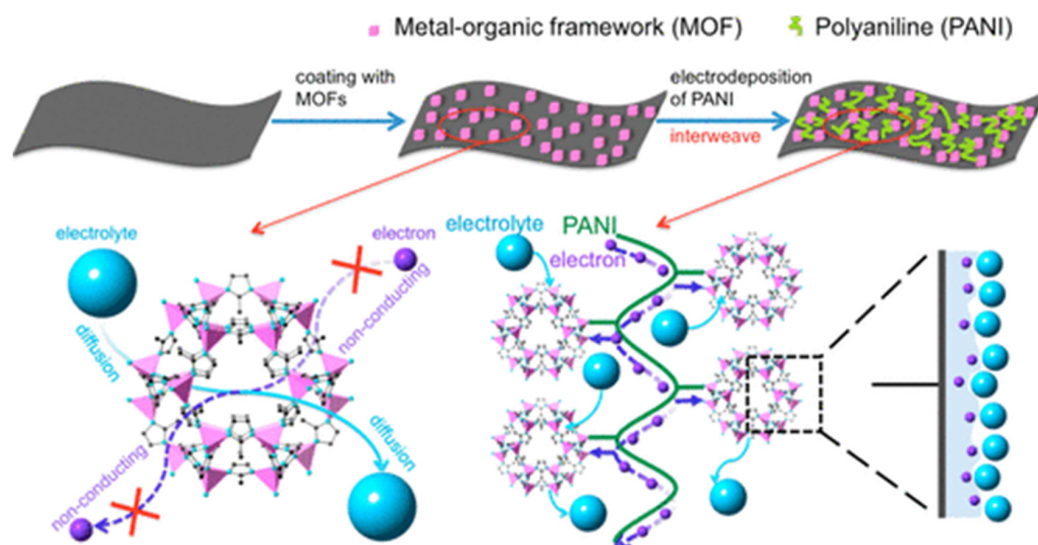
Figure 21. Preparation process for the polyaniline (PANI)–cobalt-based MOF crystals (ZIF-67)–carbon cloth (CC) for SCs applications and its conduction mechanism [100]. Reproduced with permission.

The SC performance of the prepared (PANI)-cobalt-based MOF crystals (ZIF-67)–carbon cloth (CC) electrode is as shown in Figure 22.
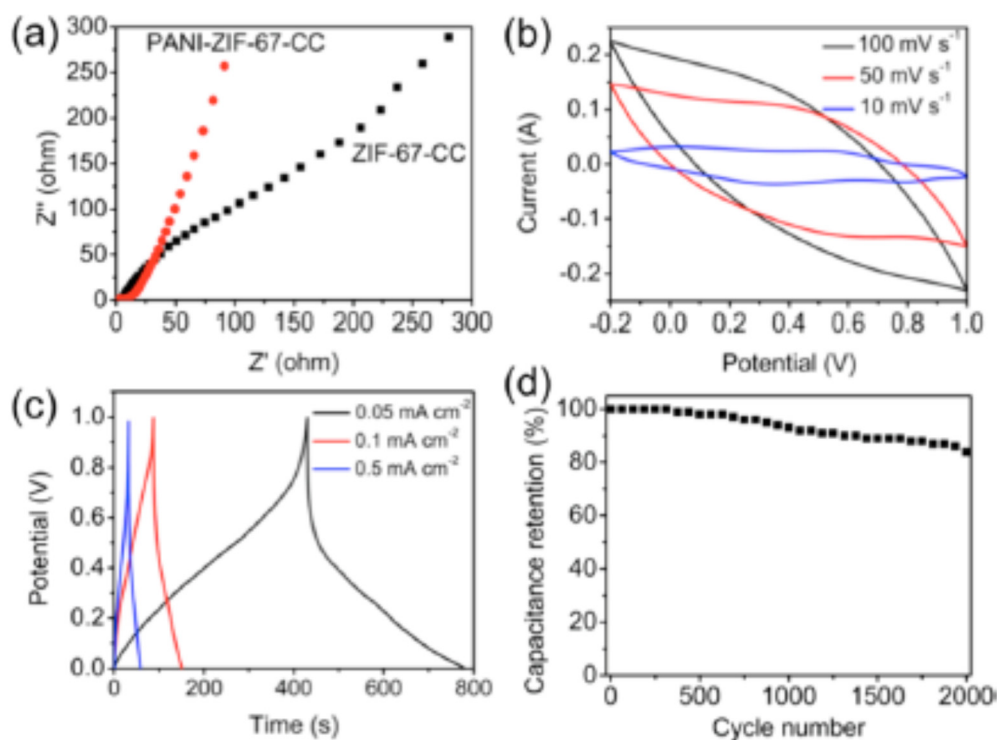
Figure 22. The SC performance of the prepared (PANI)-cobalt-based MOF crystals (ZIF-67)–carbon cloth (CC) electrode. (**a**) Nyquist electrochemical impedance spectra of ZIF-67-CC and PANI-ZIF-67-CC. (**b**) Cyclic voltammograms collected of the PANIZIF- 67-CC electrode at a different scan rate in 3MKCl. (**c**) Galvanostatic charge/discharge curves of the solid-state SC device at different current densities. (**d**) Cycling performance of the solid-state SC device measured at 0.1 mA cm^{-2} for 2000 cycles [100]. Reproduced with permission.

The flexible asymmetric supercapacitor was fabricated using Co_3O_4 as the cathode and a N-doped carbon as the anode with high robust mechanical flexibility. The 2D MOF was grown directly on the conductive substrate through thermal treatment using the "one for two" strategy [101].The electrochemical performance of Na–Zn–MOF/rGO in SC applications is shown as in Figure 23.

Figure 23. Typical examples of MOFs with assistance components for supercapacitor. (**a**) Schematic diagram of Na–Zn–MOF/rGO. (**b**) 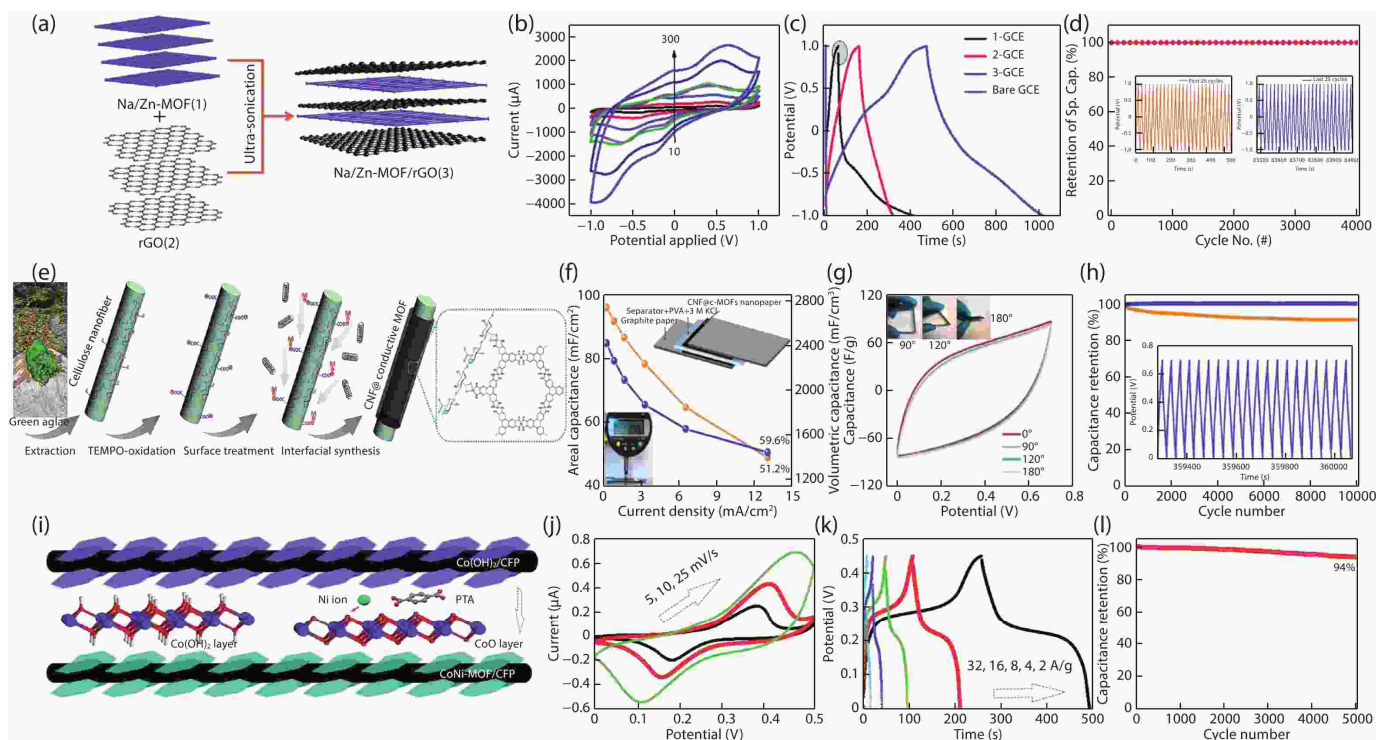The cyclic voltammograms (CV) collected of Na–Zn–MOF/rGO electrode. (**c**) A comparison of the GCD curves of a bare GCE, 1-GCE, 2-GCE, and 3-GCE. (**d**) Cycling stability analysis of Na–Zn–MOF/rGO over 4000 cycles (the left and right insets show the first and last 25 cycles). (**e**) Schematic of the synthesis procedure for the CNF@MOF hybrid nanofibers. (**f**) Calculated areal capacitances of the device at different current densities within 0–0.7 V (blue curve) and 0–1.0 V (orange curve). (**g**) The CV curves at scan rate of 100 mV/s under different folding angles. (**h**) Cyclic performance and capacitance retention data of the device within 0–0.7 V (blue curve) and 0–1.0 V (orange curve). (**i**) The schematic illustration of the strategy to synthesize CoNi–MOF/CFP. (**j**) CV curves of CoNi–MOF at a scan rate of 5, 10, and 25 mV/s. (**k**) Galvanostatic curves collected at a current density of 2, 4, 8, 16, and 32 A/g. (**l**) The cyclability of the capacitor over 5000 cycles [102]. Reproduced with permission.

The flexible-solid-state asymmetric (FASC) supercapacitor in which the Ni–MOF nanosheet was used as an electrode material exhibited the capacitances of 1518.8 F g^{-1} at 1 A g^{-1} and 244 mF cm^{-2} at 0.5 mA cm^{-2}, respectively. This supercapacitor showed excellent electrochemical stability and two LEDs can glow upto 4 min. FASC showed a long-term cycling performance and high capacitance and it has been seen that its initial capacitance of upto 97.2% can be retained even after 2000 cycles [103]. The electrochemical performance of the synthesized flexible-solid-state asymmetric (FASC) supercapacitors of the Ni–MOF and NME@Ni–MOF electrodes measured in 3.0 M KOH solution is shown in Figure 24 [104].
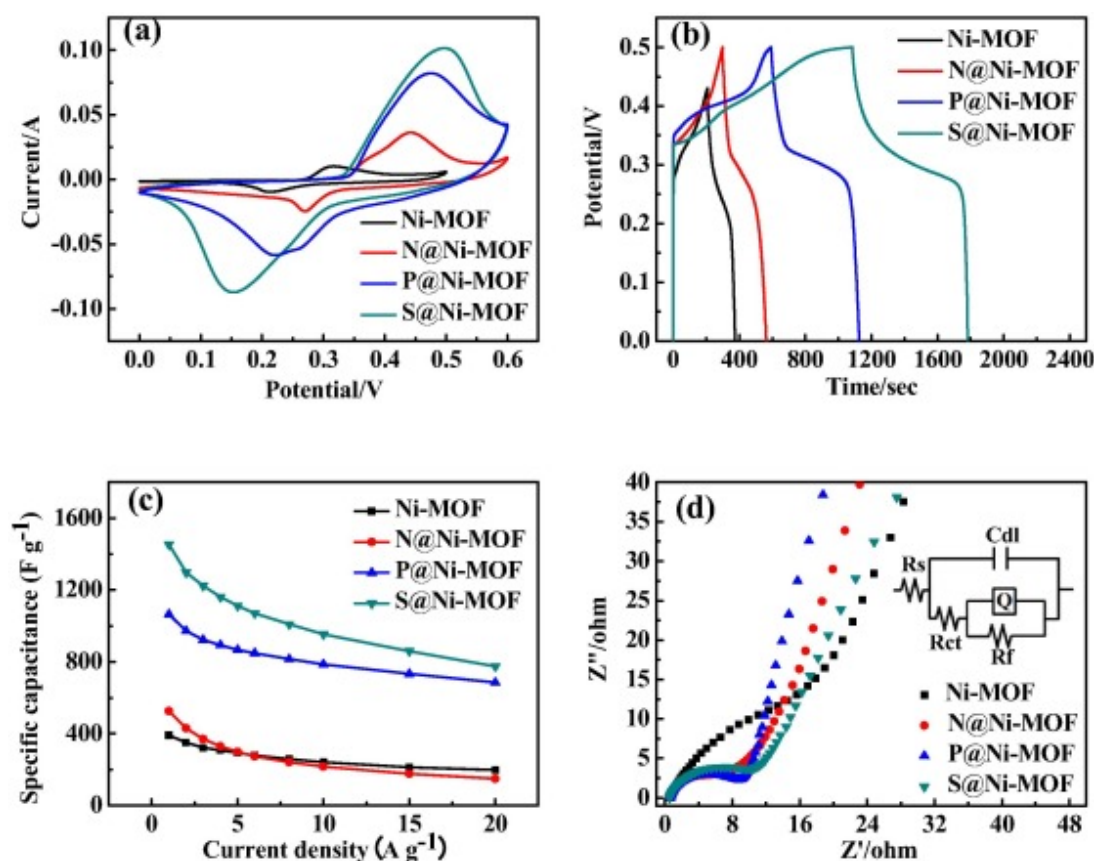
Figure 24. (**a**) CV curves of the four electrode materials measured at 30 mV s^{-1}. (**b**) GCD curves of the four electrode materials measured at 1 A g^{-1}. (**c**) The curves of the specific capacitance versus current density for four different materials. (**d**) Nyquist plots of the precursor and three composite electrode materials in 3M KOH in the frequency range of 100 kHz to 0.01 Hz. The inset is the equivalent circuit of S@Ni–MOF [104]. Reproduced with permission.

Overall, we concluded that MOFs are very interesting materials in energy storage applications and the data reported by different research groups are also summarized in Table 1.

Table 1. Different metal–organic framework in energy storage applications.

MOF Type	Current Density/ Scan Rate	Cycle Number/ Electrolyte	Capacities	Ref
Co$_3$[Co(CN)$_6$]$_2$	20 mA g^{-1}	5	304 (mAh g^{-1})	[65]
MOF-177(Zn)	50 mA g^{-1}	-	-	[65]
Co–MOF	0.6 A g^{-1}	1 M LiOH	206.76 F g^{-1}	[105]
Zr–MOF$_4$	5 mV s^{-1}	6 M KOH	207 F g^{-1}	[106]
Mo MOF-derived MoO$_3$/rGO	1 A g^{-1}	PVA−H$_2$SO$_4$	617 F g^{-1}	[107]
Ni MOF-derived nanoparticles/graphene	1 A g^{-1}	1MH$_2$SO$_4$	886 F g^{-1}	[108]
Co MOF-derived Co$_3$O$_4$ nano/microsuperstructures	1 A g^{-1}	6 M KOH	208 F g^{-1}	[109]
Mn–MOF	1 A g^{-1}	6 M KOH	443 F g^{-1}	[110]
Ni–MOF	1 A g^{-1}	3 M KOH	1057.2 F g^{-1}	[111]
MIL-101	0.25 A g^{-1}		291 F g^{-1}	[112]
Ni–MOF	10	6 M KOH	244	[113]

Table 1. *Cont.*

MOF Type	Current Density/Scan Rate	Cycle Number/Electrolyte	Capacities	Ref
Fe-MIL-88B NH$_2$	5	1 M KOH	74	[114]
Porous α-Fe$_2$O$_3$–MOF	50 cycles at a rate of 0.2 C	1.1 M LiPF$_6$ in ethylene carbonate/diethylene carbonate	424 mAh g^{-1}	[115]
Metal–organic framework-derived nanoconfinements of CoF$_2$	cyclic stability over 400 cycles.	modified LiPF$_6$/FEC/EMC electrolyte	500 mAh g^{-1}	[116]
Fe$_7$S$_8$–C/ZnS–C@MoS$_2$/rGO	5 A g^{-1}		1598.3 mA h g^{-1}	[117]
MOF-derived MnO/C nanocomposites	0.5 A g^{-1}	1 mol L^{-1} Na$_2$SO$_4$ solution	421 F g^{-1}	[118]
Ni–Co MOFs	0.5 A g^{-1}	KOH electrolyte	172.7 F g^{-1}	[119]
MOF-derived NiCo$_2$S$_4$ and carbon hybrid hollow spheres	3.8 A g^{-1}	3 M KOH and 0.02 M Zn(CH$_3$COO)$_2$ aqueous solution	343.1 mAh g^{-1}	[120]
Ni–MOF–rGO	1 ǀ A g^{-1}		272 ǀ mA g^{-1}	[121]
Co–CoO@NC/ZIF-9	0.05 mA cm^{-2}	42 cycles	(500 mAh g^{-1})	[122]

4. Conclusions

In summary, MOFs are promising precursors of a porous crystalline material, consisting of a metal atom and organic linker to prepare various advanced functional materials with the desired composition, morphology, structure, and properties. They exhibit a wide range of applications, especially in the field of energy storage and conversion including fuels, cells, batteries, and superconductors. In this review, we studied the various techniques for the synthesis of porous crystalline MOFs. Various strategies have been used by scientists, in the last few decades, for the synthesis of a variety of MOFs by changing their structural and electronic features. These MOFs in the laboratory can be synthesized using various methods including hydrothermal bombs, the heating of materials at very high temperature, and their different types of geometries have been discussed. It has also been considered that the geometry of MOFs can be controlled by altering the organic and metal ion ratios. In this way, various types of MOFs can be designed and utilized in various applications depending upon their properties.

In the second part, we discussed the various properties of MOFs, especially focusing on their energy storage devices. MOFs, because of their high porosity, high surface area, tunable pore size, and hence their structure, show great performance in energy storage devices including various kinds of batteries, fuel cells, and supercapacitors. They have excellent choices of tunable organic linkers and metals, which resulted in different nanostructures. Similarly, the performance of MOFs can be enhanced by the doping of N, O, and P, which is an effective approach. In addition, mixed transition metal oxides obtained from MOFs have attracted much attention due to their wide range of applications. Obviously, these properties can be realized from different MOFs, which lead to their superior performance because of their controllable shape, size, and structure and purity of the materials.

The new potential applications of MOFs include catalysis, gas sorption, electrochemical energy, and sensing applications. The performance can be improved by blending liquid MOFs with different materials such as glass, etc. and can be used in heterogenous catalysis chemistry. The stability and scale-up preparation of MOFs is the main challenge in this area. Additionally, these materials suffer from poor thermal, chemical, and mechanical stabilities, which might limit their practical applications.

Abbreviations

MOFs	Metal–organic frameworks
SCs	Super capacitors
LSBs	Lithium–sulfur batteries
1D	One-dimensional
2D	Two-dimensional
3D	Three-dimensional
MIL101	Metal–organic framework-101
NMOF	Nanoscale metal–organic frameworks
Cr-BDC	Chromium-benzenedicarboxylate
IRMOF	Isoreticular metal framework
MTBS	Methyltributylammonium methyl sulfate
LAG	Liquid assisted grinding
DMF	Dimethylformamide
DABCO	1,4-Diazabicyclo[2.2.2]octane
MIL-53, MIL-68, MIL-125, UiO-66, ZIF	Metal–organic frameworks
LIBs	Lithium-ion batteries
SIBs	Sulfur-ion batteries
ZnO	Zinc oxide
Li–S/Se	Lithium–sulfur/selenium batteries
H–Co–MOF	Co-based metal organic framework
EIS spectra	Electrochemical impedance spectroscopy spectra
SEI layer	Solid electrolyte interface layer
CV	Cyclic voltammetry
Ni–MOF	Nickel metal–organic frameworks
ZIF-8	2-Methylimidazole zinc salt
ZIF-C	Microporous carbon
CPC	Cube-shaped porous carbon
CNTs	Carbon nanotubes
Sb@PC	Antimony embedded porous carbon nanocomposite
3DPC	3D porous carbon
Li–O_2	Lithium–oxygen batteries
SCs	Super capacitors
EDL	Electrochemical double layer
EDLC	Electrochemical double-layer capacitance
Co8–MOF-5	Cobalt-based metal organic framework
PANI-ZIF-67-CC	Polyaniline–cobalt-based MOF crystals—carbon cloth
LEDs	Light emitting diodes
FASC	Flexible-solid-state asymmetric supercapacitor

References

1. Heo, D.Y.; Do, H.H.; Ahn, S.H.; Kim, S.Y. Metal-Organic Framework Materials for Perovskite Solar Cells. *Polymers* **2020**, *12*, 2061. [CrossRef] [PubMed]
2. Sun, Y.; Zheng, L.; Yang, Y.; Qian, X.; Fu, T.; Li, X.; Yang, Z.; Yan, H.; Cui, C.; Tan, W. Metal–Organic Framework Nanocarriers for Drug Delivery in Biomedical Applications. *Nano-Micro Lett.* **2020**, *12*, 103. [CrossRef]

3. Li, H.; Eddaoudi, M.; O'Keeffe, M.; Yaghi, O.M. Design and synthesis of an exceptionally stable and highly porous metal-organic framework. *Nature* **1999**, *402*, 276–279. [CrossRef]

4. Baumann, A.E.; Burns, D.A.; Liu, B.; Thoi, V.S. Metal-organic framework functionalization and design strategies for advanced electrochemical energy storage devices. *Commun. Chem.* **2019**, *86*, 2. [CrossRef]

5. Yaghi, O.M.; Li, H. Hydrothermal Synthesis of a Metal-Organic Framework Containing Large Rectangular Channels. *J. Am. Chem. Soc.* **1995**, *117*, 10401–10402. [CrossRef]

6. Chen, B.; Ockwig, N.W.; Millward, A.R.; Contreras, D.S.; Yaghi, O.M. High H_2 Adsorption in a Microporous Metal–Organic Framework with Open Metal Sites. *Angew. Chem. Int. Ed.* **2005**, *44*, 4745–4749. [CrossRef]

7. Rosseinsky, M.J. Enlightened pores. *Nat. Mater.* **2010**, *9*, 609–610. [CrossRef]

8. Furukawa, H.; Cordova, K.E.; O'Keeffe, M.; Yaghi, O.M. The Chemistry and Applications of Metal-Organic Frameworks. *Science* **2013**, *341*, 1230444. [CrossRef]

9. Yap, M.H.; Fow, K.L.; Chen, G.Z. Synthesis and applications of MOF-derived porous nanostructures. *Green Energy Environ.* **2017**, *2*, 218–245. [CrossRef]

10. Goodenough, J.B. Electrochemical energy storage in a sustainable modern society. *Energy Environ. Sci.* **2014**, *7*, 14–18. [CrossRef]

11. Dubal, D.P.; Ayyad, O.; Ruiz, V.; Gomez-Romero, P. Hybrid energy storage: The merging of battery and supercapacitorchemistries. *Chem. Soc. Rev.* **2015**, *44*, 1777–1790. [CrossRef] [PubMed]

12. Goodenough, J.B.; Park, K.-S. The Li-Ion Rechargeable Battery: A Perspective. *J. Am. Chem. Soc.* **2013**, *135*, 1167–1176. [CrossRef]

13. Wang, Y.; Xia, Y. Recent Progress in Supercapacitors: From Materials Design to System Construction. *Adv. Mater.* **2013**, *25*, 5336–5342. [CrossRef]

14. Shi, N.; Xi, B.; Liu, J.; Zhang, Z.; Song, N.; Chen, W.; Feng, J.; Xiong, S. Dual-Functional NbN Ultrafine Nanocrystals Enabling Kinetically Boosted Lithium–Sulfur Batteries. *Adv. Func. Mater.* **2022**, *32*, 2111586. [CrossRef]

15. Zhang, C.; Chen, Z.; Wang, H.; Nie, Y.; Yan, J. Porous Fe2O3 Nanoparticles as Lithium-Ion Battery Anode Materials. *ACS Appl. Nano Mater.* **2021**, *4*, 8744–8752. [CrossRef]

16. Liu, Z.; Yuan, X.; Zhang, S.; Wang, J.; Huang, Q.; Yu, N.; Zhu, Y.; Fu, L.; Wang, F.; Chen, Y.; et al. Three-dimensional ordered porous electrode materials for electrochemical energy storage. *NPG Asia Mater.* **2011**, *11*, 12. [CrossRef]

17. Ding, M.; Flaig, R.W.; Jiang, H.-L.; Yaghi, O.M. Carbon capture and conversion using metal-organic frameworks and MOF-based materials. *Chem. Soc. Rev.* **2019**, *48*, 2783–2828. [CrossRef]

18. Jhung, S.H.; Lee, J.H.; Chang, J.S. Microwave synthesis of a nanoporous hybrid material, chromium trimesate. *Bull. Kor. Chem. Soc.* **2005**, *26*, 880–881.

19. Taylor-Pashow, K.M.; Della Rocca, J.; Xie, Z.; Tran, S.; Lin, W. Postsynthetic modifications of iron-carboxylate nanoscale metal-organic frameworks for imaging and drug delivery. *J. Amer. Chem. Soc.* **2009**, *131*, 14261–14263. [CrossRef]

20. Khan, N.A.; Kang, I.J.; Seok, H.Y.; Jhung, S.H. Facile synthesis of nano-sized metal-organic frameworks, chromium-benzenedicarboxylate, MIL-101. *Chem. Eng. J.* **2011**, *166*, 1152–1157. [CrossRef]

21. Horcajada, P.; Chalati, T.; Serre, C.; Gillet, B.; Sebrie, C.; Baati, T.; Gref, R. Porous metal-organic-framework nanoscale carriers as a potential platform for drug delivery and imaging. *Nat. mat.* **2010**, *9*, 172–178. [CrossRef] [PubMed]

22. Tranchemontagne, D.J.; Hunt, J.R.; Yaghi, O.M. Room temperature synthesis of metal-organic frameworks: MOF-5, MOF-74, MOF-177, MOF-199, and IRMOF-0. *Tetrahedron* **2008**, *64*, 8553–8557. [CrossRef]

23. Qiu, L.G.; Li, Z.Q.; Wu, Y.; Wang, W.; Xu, T.; Jiang, X. Facile synthesis of nanocrystals of a microporous metal-organic framework by an ultrasonic method and selective sensing of organoamines. *Chem. Comm.* **2008**, *31*, 3642–3644. [CrossRef] [PubMed]

24. Schlesinger, M.; Schulze, S.; Hietschold, M.; Mehring, M. Evaluation of synthetic methods for microporous metal-organic frameworks exemplified by the competitive formation of $[Cu_2(btc)_3(H_2O)_3]$ and $[Cu_2(btc)(OH)(H_2O)]$. *Micropo. Mesop. Mat.* **2010**, *132*, 121–127. [CrossRef]

25. Mueller, U.; Schubert, M.; Teich, F.; Puetter, H.; Schierle-Arndt, K.; Pastre, J. Metal-organic frameworks-prospective industrial applications. *J. Mat. Chem.* **2006**, *16*, 626–636. [CrossRef]

26. Ameloot, R.; Stappers, L.; Fransaer, J.; Alaerts, L.; Sels, B.F.; De Vos, D.E. Patterned growth of metal-organic framework coatings by electrochemical synthesis. *Chem. Mat.* **2009**, *21*, 2580–2582. [CrossRef]

27. Ameloot, R.; Pandey, L.; Vander Auweraer, M.; Alaerts, L.; Sels, B.F.; De Vos, D.E. Patterned film growth of metal-organic frameworks based on galvanic displacement. *Chem. Comm.* **2010**, *46*, 3735–3737. [CrossRef]

28. Friščić, T.; Fábián, L. Mechanochemical conversion of a metal oxide into coordination polymers and porous frameworks using liquid-assisted grinding (LAG). *Cryst. Eng. Comm.* **2009**, *11*, 743–745. [CrossRef]

29. Liu, Y.; Wei, Y.; Liu, M.; Bai, Y.; Chen, J.; Liu., Y. Electrochemical Synthesis of Large Area Two-Dimensional Metal–Organic Framework Films on Copper Anodes. *Angew. Chem. Int. Ed.* **2020**, *59*, 1–6.

30. Yuan, W.; Friščić, T.; Apperley, D.; James, S.L. High reactivity of metal–organic frameworks under grinding conditions: Parallels with organic molecular materials. *AngewandteChemie Inter. Ed.* **2010**, *49*, 3916–3919. [CrossRef]

31. Giowniak, S.; Choma, J.; Jaroniec, M. Mechanochemistry: Toward green synthesis of metal–organic frameworks. *Mater. Today* **2021**, *46*, 109–124. [CrossRef]

32. Friscic, T.; Reid, D.G.; Halasz, I.; Stein, R.S.; Dinnebier, R.E.; Duer, M.J. Ionandliquid-assisted grinding: Improved mechanochemical synthesis of metal-organicframeworks reveal salt inclusion and anion templating. *Angew. Chem.* **2010**, *122*, 724–727. [CrossRef]

33. Loiseau, T.; Lecroq, L.; Volkringer, C.; Marrot, J.; Ferey, G.; Haouas, M.; Latroche, M. MIL-96, a porous aluminum trimesate 3D structure constructed from a hexagonalnetwork of 18-membered rings and μ 3 -oxo-centered trinuclear units. *J. Amer. Chem. Soc.* **2006**, *128*, 10223–10230. [CrossRef] [PubMed]

34. Volkringer, C.; Loiseau, T. A new indium metal-organic 3D framework with 1,3,5-benzenetricarboxylate, MIL-96 (In), containing μ^3-oxo-centered trinuclear units and a hexagonal 18-ring network. *Mat.Res.Bull.* **2006**, *41*, 948–954. [CrossRef]

35. Volkringer, C.; Loiseau, T.; Férey, G.; Morais, C.M.; Taulelle, F.; Montouillout, V.; Massiot, D. Synthesis, crystal structure and ^{71}Ga solid state NMR of a MOF-type gallium trimesate (MIL-96) with μ^3-oxo bridged trinuclear units and a hexagonal 18-ring network. *MicropoMesopo Mat.* **2007**, *105*, 111–117. [CrossRef]

36. Zhang, J.Y.; Cheng, A.L.; Yue, Q.; Sun, W.W.; Gao, E.Q. Eight coordination with bis(bidentate) bridging ligands: Zeolitic topology versus square grid networks. *Chem. Comm.* **2008**, *7*, 847–849. [CrossRef]

37. Dong, B.X.; Gu, X.J.; Xu, Q. Solvent effect on the construction of two microporous yttrium-organic frameworks with high thermostability via in situ ligand hydrolysis. *Dalton Trans.* **2010**, *39*, 5683–5687. [CrossRef]

38. Nadeem, M.A.; Thornton, A.W.; Hill, M.R.; Stride, J.A. A flexible copper based microporous metal-organic framework displaying selective adsorption of hydrogen over nitrogen. *Dalton Trans.* **2011**, *40*, 3398–3401. [CrossRef]

39. Bauer, S.; Serre, C.; Devic, T.; Horcajada, P.; Marrot, J.; Férey, G.; Stock, N. High-throughput assisted rationalization of the formation of metal organic frameworks in the iron (III) aminoterephthalate solvothermal system. *Inorg. Chem.* **2008**, *47*, 7568–7576. [CrossRef]

40. Ahnfeldt, T.; Guillou, N.; Gunzelmann, D.; Margiolaki, I.; Loiseau, T.; Ferey, G.; Stock, N. [Al$_4$ (OH)$_2$ (OCH$_3$)$_4$ (H$_2$N-bdc)$_3$]·xH$_2$O: A 12-Connected Porous Metal-OrganicFramework with an Unprecedented Aluminum-Containing Brick. *Angew. Chem. Intern. Edi.* **2009**, *48*, 5163–5166. [CrossRef]

41. Long, P.; Wu, H.; Zhao, Q.; Wang, Y.; Dong, J.; Li, J. Solvent effect on the synthesis of MIL-96 (Cr) and MIL-100 (Cr). *Micropo. Mesopo. Mat.* **2011**, *142*, 489–493. [CrossRef]

42. Dunn, B.; Kamath, H.; Tarascon, J.-M. Electrical Energy Storage for the Grid: A Battery of Choices. *Science* **2011**, *334*, 928–935. [CrossRef] [PubMed]

43. Seh, Z.W.; Kibsgaard, J.; Dickens, C.F.; Chorkendorff, I.; Norskov, J.K.; Jaramillo, T.F. Combining theory and experiment in electrocatalysis: Insights into materials design. *Science* **2017**, *355*, 1–12. [CrossRef] [PubMed]

44. Merlet, C.; Rotenberg, B.; Madden, P.A.; Taberna, P.-L.; Simon, P.; Gogotsi, Y.; Salanne, M. On the molecular origin of supercapacitance in nanoporous carbon electrodes. *Nat. Mater.* **2012**, *11*, 306–310. [CrossRef]

45. Lin, M.-C.; Gong, M.; Lu, B.; Wu, Y.; Wang, D.-Y.; Guan, M.; Angell, M.; Chen, C.; Yang, J.; Hwang, B.-J.; et al. An ultrafast rechargeable aluminium-ion battery. *Nature* **2015**, *520*, 324–328. [CrossRef] [PubMed]

46. Liu, J.; Zhang, J.-G.; Yang, Z.; Lemmon, P.J.; Imhoff, C.; Graff, G.L.; Li, L.; Hu, J.; Jie, X.; Xia, G.; et al. Materials Science and Materials Chemistry for Large Scale Electrochemical Energy Storage: From Transportation to Electrical Grid. *Adv. Funct. Mater.* **2013**, *23*, 929–946. [CrossRef]

47. Yabuuchi, N.; Kubota, K.; Dahbi, M.; Komaba, S. Research development on sodium-ion batteries. *Chem. Rev.* **2014**, *114*, 11636–11682. [CrossRef]

48. Kubota, K.; Komaba, S. Practical issues and future perspective for Na-ion batteries. *J.Electrochem. Soc.* **2015**, *162*, A2538–A2550. [CrossRef]

49. Nithya, C.; Gopukumar, S. Sodium ion batteries: A newer electrochemical storage. *WIREs Energy Environ.* **2015**, *4*, 253–278. [CrossRef]

50. Han, M.H.; Gonzalo, E.; Singh, G.; Rojo, T. A comprehensive review of sodium layered oxides: Powerful cathodes for Na-ion batteries. *Energy Environ. Sci.* **2015**, *8*, 81–102. [CrossRef]

51. Kundu, D.; Talaie, E.; Duffort, V.; Nazar, L.F. The Emerging Chemistry of Sodium Ion Batteries for Electrochemical Energy Storage. *Angew. Chem. Int. Ed.* **2015**, *54*, 3431–3448. [CrossRef]

52. Jiang, H.; Lee, P.S.; Li, C. 3D carbon based nanostructures for advanced supercapacitors. *Energy Environ. Sci.* **2013**, *6*, 41–53.

53. Reinsch, H.; van der Veen, M.A.; Gil, B.; Marszalek, B.; Verbiest, T.; de Vos, D.; Stock, N. Structures, Sorption Characteristics, and Nonlinear Optical Properties of a New Series of Highly Stable Aluminum MOFs. *Chem. Mater.* **2013**, *25*, 17–26. [CrossRef]

54. Canivet, J.; Bonnefoy, J.; Daniel, C.; Legrand, A.; Coasne, B.; Farrusseng, D. Structure–property relationships of water adsorption in metal–organic frameworks. *New J. Chem.* **2014**, *38*, 3102–3111. [CrossRef]

55. Fletcher, A.J.; Thomas, K.M.; Rosseinsky, M.J. Flexibility in metal-organic framework materials: Impact on sorption properties. *J. Solid State Chem.* **2005**, *178*, 2491–2510. [CrossRef]

56. Canivet, J.; Bonnefoy, J.; Daniel, C.; Legrand, A.; Coasne, B.; Farrusseng, D. Metal–organic framework structure–property relationships for high-performance multifunctional polymer nanocomposite applications. *J. Mater. Chem. A* **2021**, *9*, 4348–4378.

57. Eddaudi, M.; Kim, J.; Rosi, N.; Vodak, D.; Wachter, J.; O'Keeffe, M.; Yaghi, O.M. Systematic Design of Pore Size and Functionality in Isoreticular MOFs and Their Application in Methane Storage. *Science* **2002**, *295*, 469–472. [CrossRef] [PubMed]

58. Sun, L.; Hendon, C.H.; Minie, M.A.; Walsh, A.; Dincă, M. Million-Fold Electrical Conductivity Enhancement in Fe$_2$(DEBDC) versus Mn$_2$(DEBDC) (E = S, O). *J. Am. Chem. Soc.* **2015**, *137*, 6164–6167. [CrossRef]

59. Kim, S.; Joarder, B.; Hurd, J.A.; Zhang, J.; Dawson, K.W.; Gelfand, B.S.; Wong, N.E.; Shimizu, G.K.H. Achieving Superprotonic Conduction in Metal–Organic Frameworks through Iterative Design Advances. *J. Am. Chem. Soc.* **2018**, *140*, 1077–1082. [CrossRef]

60. Zhou, J.; Li, R.; Fan, X.; Chen, Y.; Han, R.; Li, W.; Zheng, J.; Wang, B.; Li, X. Rational design of a metal–organic framework host for sulfur storage in fast, long-cycle Li–S batteries. *Energy Environ. Sci.* **2014**, *7*, 2715–2724. [CrossRef]

61. Xu, G.; Nie, P.; Dou, H.; Ding, B.; Li, L.; Zhang, X. Exploring metal organic frameworks for energy storage in batteries and supercapacitors. *Mater. Today* **2017**, *20*, 191–209. [CrossRef]

62. Ferey, G.; Millange, F.; Morcrette, M.; Serre, C.; Doublet, M.-L.; Greneche, J.-M.; Tarascon, J.-M. Mixed-valence li/fe-based metal-organic frameworks with both reversible redox and sorption properties. *Angew. Chem. Int. Ed.* **2007**, *46*, 3259–3263. [CrossRef] [PubMed]

63. Chen, L.; Yang, W.; Wang, J.; Chen, C.; Wei, M. Hierarchical Cobalt-Based Metal-Organic Framework for High-Performance Lithium-Ion Batteries. *Chem.-A Eurpean J.* **2018**, *24*, 13362–13367. [CrossRef] [PubMed]

64. Ren, J.; Huang, Y.; Zhu, H.; Zhang, B.; Zhu, H.; Shen, S.; Tan, G.; Wu, F.; He, H.; Lan, S.; et al. Recent progress on MOF-derived carbon materials forenergy storage. *Carbon Energy* **2020**, *2*, 176–202. [CrossRef]

65. Li, X.; Cheng, F.; Zhang, S.; Chen, J. Shape-controlled synthesis and lithium-storage study of metal-organic frameworks $Zn_4O(1,3,5-benzenetribenzoate)_2$. *J. Power Sources* **2006**, *160*, 542–547. [CrossRef]

66. Lu, S.; Wang, H.; Zhou, J.; Wu, X.; Qin, W. Atomic layer deposition of ZnO on carbon black as nanostructured anode materials for high-performance lithium-ion batteries. *Nanoscale* **2017**, *9*, 1184–1192. [CrossRef]

67. Song, Y.; Chen, Y.; Wu, J.; Fu, Y.; Zhou, R.; Chen, S.; Wang, L. Hollow metal organic frameworks-derived porous ZnO/C nanocages as anode materials for lithium-ion batteries. *J. Alloy. Compd.* **2017**, *694*, 1246–1253. [CrossRef]

68. Huang, P.-B.; Tian, L.-Y.; Zhang, Y.-H.; Shi, F.-N. Facile synthesis of polymetallic Li-MOFs and their synergistic mechanism of lithium storage. *Inorg. Chim. Acta* **2021**, *525*, 120473. [CrossRef]

69. An, T.; Wang, Y.; Tang, J.; Wang, Y.; Zhang, L.; Zheng, G. A flexible ligand-based wavy layered metal–organic framework for lithium-ion storage. *J. Colloid Interface Sci.* **2015**, *445*, 320–325. [CrossRef]

70. Park, G.D.; Kang, Y.C. One-Pot Synthesis of $CoSe_x$–rGO Composite Powders by Spray Pyrolysis and Their Application as Anode Material for Sodium-Ion Batteries. *Chem. Eur. J.* **2016**, *22*, 4140–4146. [CrossRef]

71. Zhang, Y.; Pan, A.; Ding, L.; Zhou, Z.; Wang, Y.; Niu, S.; Liang, S.; Cao, G. Nitrogen-Doped Yolk-Shell-Structured CoSe/C Dodecahedra for High-Performance Sodium Ion Batteries. *ACS Appl. Mater. Interfaces* **2017**, *9*, 3624–3633. [CrossRef] [PubMed]

72. Zhao, Y.; Gao, X.; Gao, H.; Dolocan, A.; Goodenough, J.B. Elevating Energy Density for Sodium-Ion Batteries through Multielectron Reactions. *Nano Lett.* **2021**, *21*, 2281–2287. [CrossRef] [PubMed]

73. Su, H.; Jaffer, S.; Yu, H. Transition metal oxides for sodium-ion batteries. *Energy Storage Materials* **2016**, *5*, 116–131. [CrossRef]

74. Wenzel, S.; Hara, T.; Janek, J.; Adelhelm, P. Room-temperature sodium-ion batteries: Improving the rate capability of carbon anode materials by templating strategies. *Energy Environ. Sci.* **2011**, *4*, 3342–3345. [CrossRef]

75. Tran, V.A.; Do, H.H.; Ha, T.D.C.; Ahn, S.H.; Kim, M.-G.; Kim, Y.S.; Lee, S.-W. Metal-organic framework for lithium and sodium-ion batteries: Progress and perspectivez. *Fuel* **2022**, *319*, 123856. [CrossRef]

76. Zhu, K.J.; Liu, G.; Wang, Y.J.; Liu, J.; Li, S.T.; Yang, L.Y.; Liu, S.L.; Wang, H.; Xie, T. Metal-Organic Frameworks derived novel hierarchical durian-like nickel sulfide (NiS_2) as an anode material for high-performance sodium-ion batteries. *Mater. Lett.* **2017**, *197*, 180–183. [CrossRef]

77. Qu, Q.; Yun, J.; Wan, Z.; Zheng, H.; Gao, T.; Shen, M.; Shao, J.; Zheng, H. MOF-derived microporous carbon as a better choice for Na-ion batteries than mesoporous CMK-3. *RSC Adv.* **2014**, *4*, 64692–64697. [CrossRef]

78. Choi, D.; Lim, S.; Han, D. Advanced metal–organic frameworks for aqueous sodium-ion rechargeable batteries. *J. Energy Chem.* **2021**, *53*, 396–406. [CrossRef]

79. Zou, G.; Jia, X.; Huang, Z.; Li, S.; Liao, H.; Hou, H.; Huang, L.; Ji, X. Cube-shaped Porous Carbon Derived from MOF-5 as Advanced Material for Sodium-Ion Batteries. *Electro. Chim. Acta* **2016**, *196*, 413–421. [CrossRef]

80. Nie, P.; Shen, L.; Pang, G.; Zhu, Y.; Xu, G.; Qing, Y.; Dou, H.; Zhang, X. Flexible metal–organic frameworks as superior cathodes for rechargeable sodium-ion batteries. *J. Mater. Chem. A* **2015**, *3*, 16590–16597. [CrossRef]

81. Yang, G.; Luo, X.-X.; Liu, Y.; Li, K.; Wu, X.-L. [Co3(μ3-O)]-Based Metal-Organic Frameworks as Advanced Anode Materials in K- and Na-Ion Batteries. *ACS Appl. Mater. Interfaces* **2021**, *13*, 46902–46908. [CrossRef]

82. Dong, C.; Xu, L. Cobalt- and Cadmium-Based Metal-Organic Frameworks as High-Performance Anodes for Sodium Ion Batteries and Lithium Ion Batteries. *ACS Appl. Mater. Interfaces* **2017**, *9*, 7160–7168. [CrossRef] [PubMed]

83. Zhang, X.; Wang, M.; Zhu, G.; Li, D.; Yan, D.; Lu, T.; Pan, L. Porous cake-like TiO_2 derived from metal-organic frameworks as superior anode material for sodium ion batteries. *Ceram. Int.* **2017**, *43*, 2398–2402. [CrossRef]

84. Yang, H.; Kruger, P.E.; Telfer, S.G. Metal–Organic Framework Nanocrystals as Sacrificial Templates for Hollow and Exceptionally Porous Titania and Composite Materials. *Inorg. Chem.* **2015**, *54*, 9483–9490. [CrossRef]

85. Li, Q.; Zhang, W.; Peng, J.; Zhang, W.; Liang, Z.; Wu, J.; Feng, J.; Li, H.; Huang, S. Metal–Organic Framework Derived Ultrafine Sb@Porous Carbon Octahedron via In Situ Substitution for High-Performance Sodium-Ion Batteries. *ACS Nano* **2021**, *15*, 15104–15113. [CrossRef]

86. Gao, X.; Zhu, G.; Zhang, X.; Hu, T. Porous carbon materials derived from in situ construction of metal-organic frameworks for high-performance sodium ions batteries. *Microporous Mesoporous Mater.* **2019**, *273*, 156–162. [CrossRef]

87. Guo, Y.; Zhu, Y.; Yuan, C.; Wang, C. $MgFe_2O_4$ hollow microboxes derived from metal-organic-frameworks as anode material for sodium-ion batteries. *Mater. Lett.* **2017**, *199*, 101–104. [CrossRef]

88. Ji, X.; Nazar, L.F. Advances in Li–S batteries. *J. Mater. Chem.* **2010**, *20*, 9821–9826. [CrossRef]

89. Yuan, N.; Sun, W.; Yang, J.; Gong, X.; Liu, R. Multifunctional MOF-Based Separator Materials for Advanced Lithium–Sulfur Batteries. *Adv. Mater. Interfaces* **2021**, *8*, 2001941. [CrossRef]

90. Tian, H.; Tian, H.; Wang, S.; Chen, S.; Zhang, F.; Song, L.; Liu, H.; Liu, J.; Wang, G. High-power lithium–selenium batteries enabled by atomic cobalt electrocatalyst in hollow carbon cathode. *Nat. Commun.* **2020**, *11*, 5025. [CrossRef]

91. Choi, K.M.; Jeong, H.M.; Park, J.H.; Zhang, Y.B.; Kang, J.K.; Yaghi, O.M. Supercapacitors of Nanocrystalline Metal–Organic Frameworks. *ACS Nano* **2014**, *7*, 7451−7457. [CrossRef]

92. Simon, P.; Gogotsi, Y. Materials for electrochemical capacitors. *Nat. Mater.* **2008**, *7*, 845–854. [CrossRef] [PubMed]

93. Sheberla, D.; Bachman, J.C.; Elias, J.S.; Sun, C.J.; Horn, Y.S.; Dincă, M. Conductive MOF electrodes for stable supercapacitors with high areal capacitance. *Nat. Mater.* **2017**, *16*, 220–224. [CrossRef] [PubMed]

94. Salunkhe, R.R.; Kamachi, Y.; Torad, N.L.; Hwang, S.M.; Sun, Z.; Dou, S.X.; Kim, J.H.; Yamauchi, Y. Fabrication of symmetric supercapacitors based on MOF-derived nanoporous carbons. *J. Mater. Chem. A* **2014**, *2*, 19848–19854. [CrossRef]

95. Shalini, S.S.; Balamurugan, R.; Velmathi, S.; Bose, A.C. Systematic Investigation on the Electrochemical Performance of Pristine Silver Metal–Organic Framework as the Efficient Electrode Material for Supercapacitor Application. *Energy Fuels* **2022**, *36*, 7104–7114. [CrossRef]

96. Jiao, Y.; Pei, J.; Chen, D.; Yan, C.; Hu, Y.; Zhang, Q.; Chen, G.J. Mixed-metallic MOF based electrode materials for high performance hybrid supercapacitors. *Mater. Chem. A* **2017**, *5*, 1094–1102. [CrossRef]

97. He, D.; Gao, Y.; Yao, Y.; Wu, L.; Zhang, J.; Huang, Z.H.; Wang, M.X. Asymmetric Supercapacitors Based on Hierarchically Nanoporous Carbon and $ZnCo_2O_4$ From a Single Biometallic Metal-Organic Frameworks (Zn/Co-MOF). *Front. Chem.* **2020**, *8*, 1–11. [CrossRef]

98. Díaz, R.; Orcajo, M.G.; Botas, J.A.; Calleja, G.; Palma, J. Co8-MOF-5 as electrode for supercapacitors. *Mater. Lett.* **2012**, *68*, 126–128. [CrossRef]

99. Wang, L.; Feang, X.; Ren, L.; Piao, Q.; Wang, Y.; Li, H.; Wang, B. Flexible Solid-State Supercapacitor Based on a Metal–Organic Framework Interwoven by Electrochemically-Deposited PANI. *J. Am. Chem. Soc.* **2015**, *137*, 4920–4923. [CrossRef]

100. Guan, C.; Zhao, W.; Hu, Y.; Lai, Z.; Li, X.; Sun, S.; Zhang, H.; Cheetam, A.K.; Wang, J. Cobalt oxide and N-doped carbon nanosheets derived from a single two-dimensional metal–organic framework precursor and their application in flexible asymmetric supercapacitors. *NanoscaleHoriz* **2017**, *2*, 99–105. [CrossRef]

101. Wang, H.; Zhang, N.; Li, S.; Ke, Q.; Li, Z.; Zhou, M. Metal-organic framework composites for energy conversion and storage. *J. Semicond.* **2020**, *41*, 091707. [CrossRef]

102. Yang, C.; Li, X.; Yu, L.; Liu, X.; Yang, J.; Wai, M. A new promising Ni-MOF superstructure for high-performance supercapacitors. *Chem. Commun.* **2020**, *56*, 1803–1806.

103. Yue, L.; Guo, H.; Wang, X.; Sun, T.; Liu, H.; Li, Q.; Xu, M.; Yang, Y.; Yang, W. Non-metallic element modified metal-organic frameworks as high-performance electrodes for all-solid-state asymmetric supercapacitors. *J. Colloid Interface Sci.* **2018**, *539*, 370–378. [CrossRef] [PubMed]

104. Nie, P.; Shen, L.; Luo, H.; Ding, B.; Xu, G.; Wang, J.; Zhang, X. Prussian blue analogues: A new class of anode materials for lithium ion batteries. *J. Mater. Chem. A* **2014**, *2*, 5852. [CrossRef]

105. Lee, D.; Yoon, S.; Shrestha, N.; Lee, S.; Ahn, H.; Han, S. Unusual energy storage and charge retention in Co-based metal–organicframeworks. *Microporous Mesoporous Mater.* **2012**, *153*, 163–165. [CrossRef]

106. Tan, Y.; Zhang, W.; Gao, Y.; Wu, J.; Tang, B. Facile synthesis and supercapacitive properties of Zr-metal organic frameworks (UiO-66). *RSC Adv.* **2015**, *5*, 17601–17605. [CrossRef]

107. Cao, X.; Zheng, B.; Shi, W.; Yang, J.; Fan, Z.; Luo, Z.; Rui, X.; Chen, B.; Yan, Q.; Zhang, H. Reduced Graphene Oxide-Wrapped MoO_3Composites Prepared by Using Metal-Organic Frameworks as Precursor for All-Solid-State Flexible Supercapacitors. *Adv. Mater.* **2015**, *27*, 4695–4701. [CrossRef] [PubMed]

108. Wu, M.S.; Hsu, W.H. Nickel nanoparticles embedded in partially graphitic porous carbon fabricated by direct carbonization of nickel-organic framework for high-performance supercapacitors. *J. Power Sources* **2015**, *274*, 1055–1062. [CrossRef]

109. Zhang, F.; Hao, L.; Zhang, L.; Zhang, X. Solid-state thermolysis preparation of Co_3O_4 nano/micro superstructures from metal-organic framework for supercapacitors. *Int. J. Electrochem. Sci.* **2011**, *6*, 2943–2954.

110. Feng, C.; Lv, C.P.; Zhao, H.; Li, Z.Q.; Xie, W.N.; Sun, L.N.; Wang, Y. Structural Elucidation and Supercapacitive Performance on a Mn(II)-Based MOF. *Cryst. Growth Des.* **2020**, *20*, 5682–5687. [CrossRef]

111. Du, P.; Dong, Y.; Liu, C.; Wei, W.; Liu, D.; Liu, P. Fabrication of Hierarchical Porous Nickel Based Metal-Organic Framework (Ni-MOF) Constructed with Nanosheets as Novel Pseudo-Capacitive Material for Asymmetric Supercapacitor. *J. Colloid Interf. Sci.* **2018**, *518*, 57–68. [CrossRef] [PubMed]

112. Ullah, S.; Khan, I.A.; Choucair, M.; Badshah, A.; Khan, I.; Nadeem, M.A. A novel Cr_2O_3-carbon composite as a high performance pseudo-capacitor electrode material. *Electrochimica Acta* **2015**, *171*, 142–149. [CrossRef]

113. Han, Y.; Zhang, S.; Shen, N.; Li, D.; Li, X. MOF-Derived Porous NiO Nanoparticle Architecture for High Performance Supercapacitors. *Mater. Lett.* **2017**, *188*, 1–4. [CrossRef]

114. Meng, W.; Chen, W.; Zhao, L.; Huang, Y.; Zhu, M.; Huang, Y.; Fu, Y.; Geng, F.; Yu, J.; Chen, X.; et al. Porous Fe_3O_4/Carbon Composite Electrode Material Prepared from Metal-Organic Framework Template and Effect of Temperature on Its Capacitance. *Nano Energy* **2014**, *8*, 133–140. [CrossRef]

115. Xu, X.; Cao, R.; Jeong, S.; Cho, J. Spindle-like Mesoporous α-Fe2O3 Anode Material Prepared from MOF Template for High-Rate Lithium Batteries. *Nano Lett.* **2012**, *12*, 4988–4991. [CrossRef] [PubMed]

116. Wu, F.; Srot, V.; Chen, S.; Zhang, M.; Aken, P.A.; Wang, Y.; Maier, J.; Yu, Y. Metal–Organic Framework-Derived Nanoconfinements of CoF_2 and Mixed-Conducting Wiring for High-Performance Metal Fluoride-Lithium Battery. *ACS Nano* **2021**, *15*, 1509–1518. [CrossRef]

117. Xu, L.; Gong, Z.; Qiu, Y.; Sheng, X. Superstructure MOF as a framework to composite MoS_2 with rGO for Li/Na-ion battery storage with high-performance and stability. *Dalton Trans.* **2022**, *51*, 3472–3484. [CrossRef]

118. Qiao, Y.; Li, N.; Dong, M.; Jia, P.; Ma, C.; Zhang, T.; Jiao, T. MOF-Derived MnO/C Nanocomposites for High-Performance Supercapacitors. *Nanomaterials* **2022**, *12*, 4257. [CrossRef]

119. Ye, C.; Quin, Q.; Liu, J.; Mao, W.; Yan, J.; Wu, Y. Coordination derived stable Ni–Co MOFs for foldable all-solid-state supercapacitors with high specific energy. *J. Mater. Chem. A* **2019**, *7*, 4998–5008. [CrossRef]

120. Yu, J.; Cai, D.; Si, J.; Zhang, H.; Wang, Q. MOF-derived $NiCo_2S_4$ and carbon hybrid hollow spheres compactly concatenated by electrospun carbon nanofibers as self-standing electrodes for aqueous alkaline Zn batteries. *J. Mater. Chem. A* **2022**, *10*, 4100–4109. [CrossRef]

121. Haroon, H.; Wahid, M.; Majid, K. Structure-Activity Relationships of a Ni-MOF, a Ni-MOF-rGO, and pyrolyzed Ni/C@rGO Structures for Sodium- ion Batteries. *Chem. Sel.* **2022**, *7*, e202202011. [CrossRef]

122. Chen, X.; Chen, C.; Zhang, X.; Huang, T.; Yu, A. Mesoporous Co–CoO@NC Micro-Disk Derived from ZIF-9 as Bifunctional Catalyst for Lithium-Oxygen Batteries. *Chem. Sel.* **2018**, *3*, 9276–9283. [CrossRef]